The CERN Accelerator School

Physical Properties and Testing

3 June 2024

Dr. Ana Arauzo

University of Zaragoza

CSIC Consejo Superior de Investigaciones Científicas

Universidad Zaragoza 1542

INMA Instituto de Nanociencia y Materiales de Aragón

Outline

- Introduction
  - Physical Properties of materials in accelerator applications.
  - University of Zaragoza labs
- Electrical Properties of Materials:
  - $R(T)$, RRR, T_c
  - Testing Methods and standards
  - Examples
- Thermal Properties:
  - $c_P(T,H)$, $k(T)$
  - Testing methods
  - Examples: Nitronic 50 austenitic steel
- Magnetic Properties,
  - M(H), $\mu_r(H)$
  - Hysteresis main parameters
  - Testing Methods and standards
  - Examples: Non magnetic alloys, magnetic steel, manufacturing

Introduction

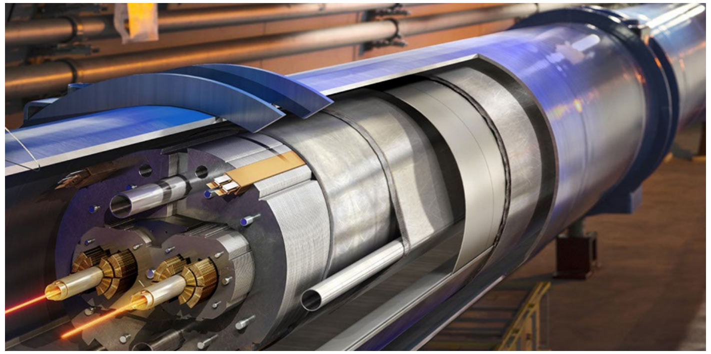

Physical Properties of materials at extreme conditions

High Radiation dose (accumulative damage)
Very low T (1.9K superfluid LHe)
High T gradients
High Magnetic Fields (8.3 T ≈ $2\cdot10^5$ B_{Earth})
High vacuum

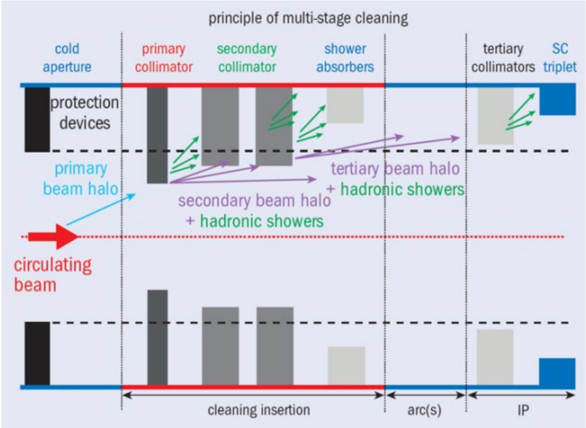

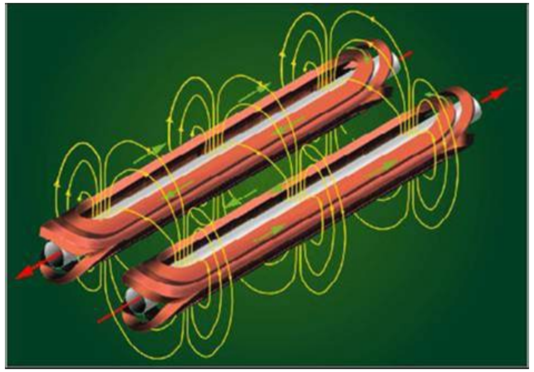

Robust carbon-fibre composites and non-robust but high-absorption metallic materials (W) are used

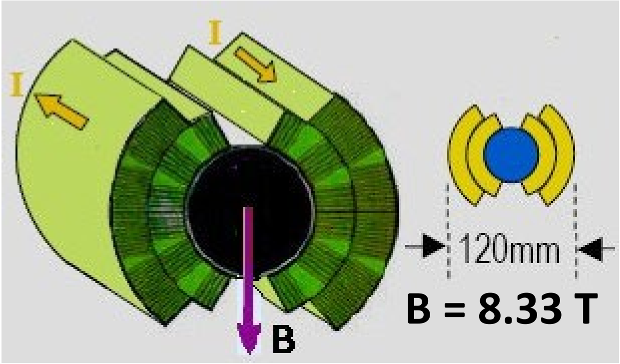

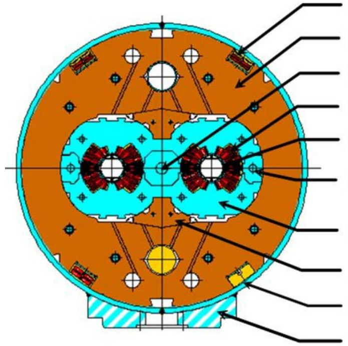

Introduction

Physical Properties of materials at extreme conditions

Electrical Properties of Materials:
-Resistivity, electrical transport

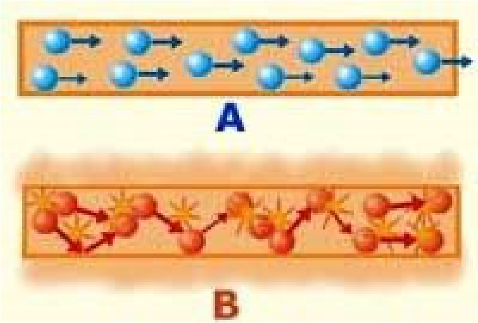

Thermal Properties:
- Heat capacity
- Thermal conductivity

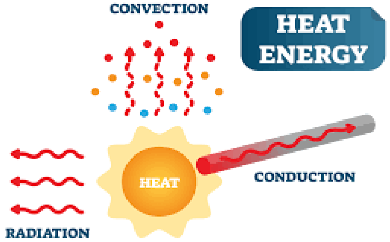

Magnetic Properties

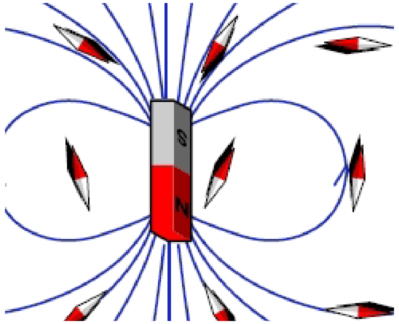

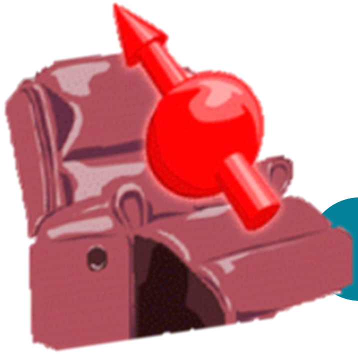

Cryogenic Temperatures: $T < 10$ K
High Magnetic Fields: $B > 2$ T

Introduction

The CERN Accelerator School

Physical Properties of materials at extreme conditions: low *T*, high *H*

UZ Research Labs

Physical Properties Measurement System: PPMS-14T

1.9 K – 400 K

14T Magnetic field

Electrical Properties of Materials
Thermal Properties:
Magnetic Properties

PPMS with ^{3}He refrigerator

350 K – 0.35 K

- Heat Capacity
- Resistivity DC
- Electrical transport ACT

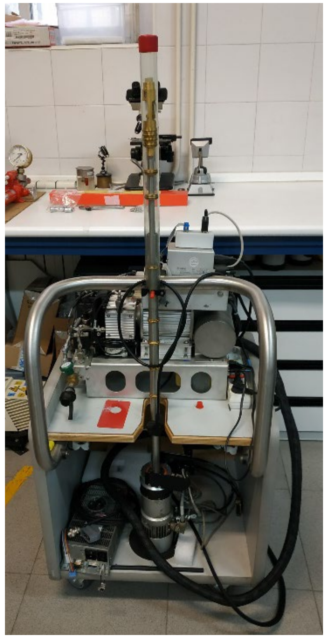

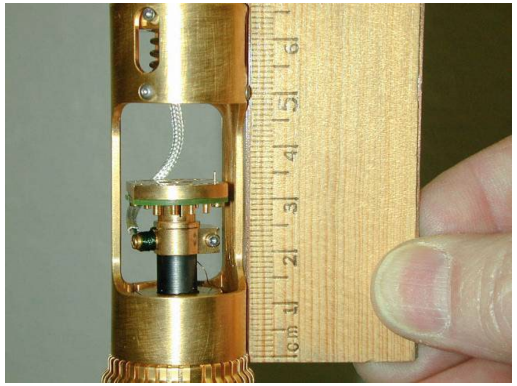

Sample stage

Universidad Zaragoza

Introduction

The CERN Accelerator School

Physical Properties of materials at extreme conditions: low *T*, high *H*

UZ Research Labs

SQUID Magnetometer MPMS3

7T Magnet

EQC2021-007030-P. *Magnetómetro SQUID Sub-K*. Funding Agency: European Union, NextGenerationEU funds. EQC2021 call. 854 k€.

- Options for Standard *T* : 1.8 – 400 K
  - VSM/DC mode
  - AC measurement system

  0.1 Hz – 1000 Hz
  - Rotator – single crystal
  - Fiber optic – Magneto-optic
  - Pressure Cell

Introduction

The CERN Accelerator School

Physical Properties of materials at extreme conditions: low *T*, high *H*

UZ Research Labs

Sub-K SQUID Magnetometer MPMS3

Extending the Temperature Range

Helium-3 Refrigerator

- 2 K – 0.4K

Zaragoza

Electrical Properties of Materials

Ohm's Law: $R=V/I$

$\rho = RA/L$

The resistivity, ρ, is independent of specimen geometry

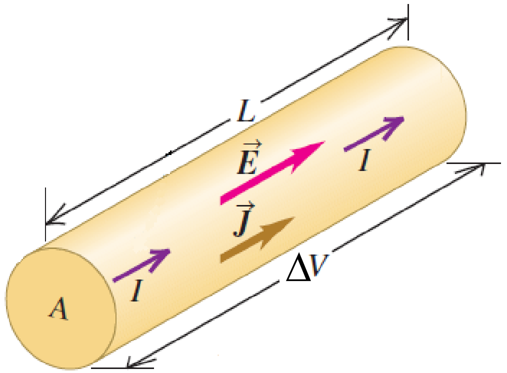

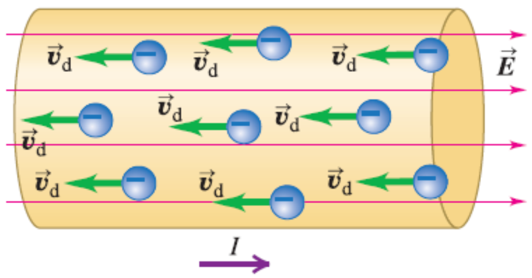

Classical view

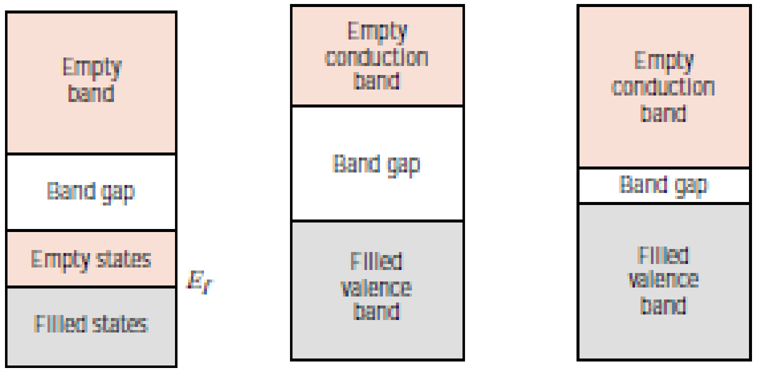

Metals Insulators Semiconductors

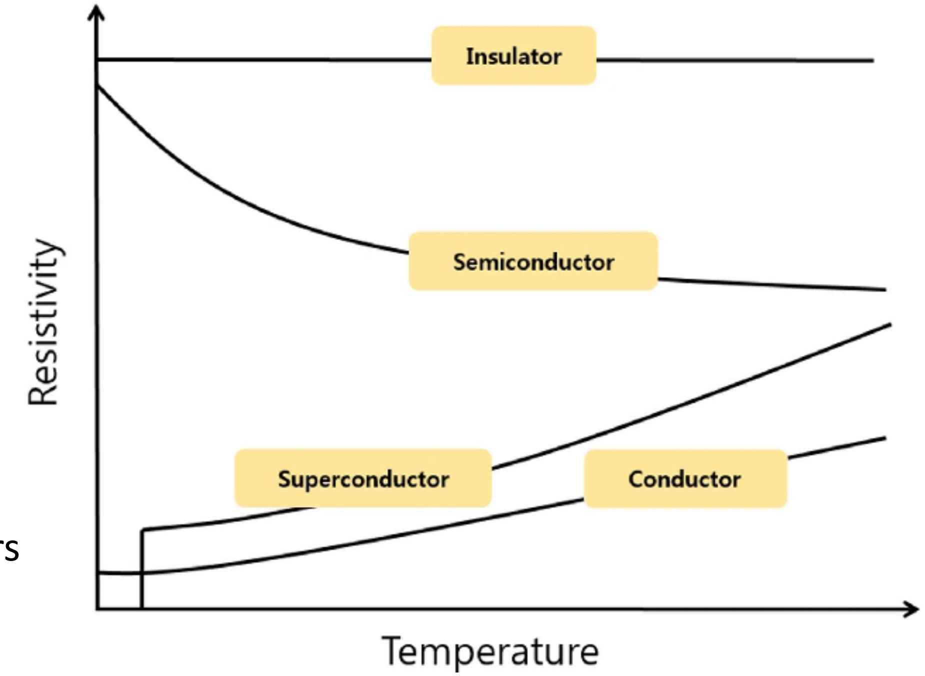

The electrical properties of a solid material are a consequence of its electron band structure

Electrical Properties of Materials: metals

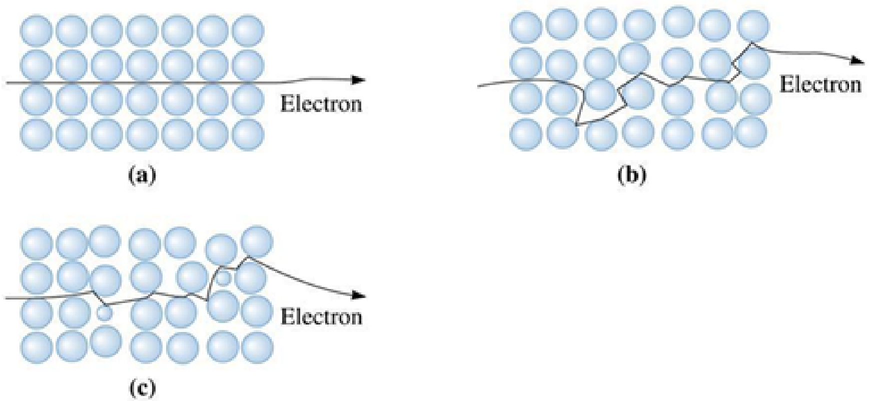

Figure (1): Movement of an electron through (a) a perfect crystal, (b) a crystal heated to a high temperature, and (c) a crystal containing atomic level defects. Scattering of the electrons reduces the mobility and conductivity.

$$\rho_t = \rho_0 + aT$$

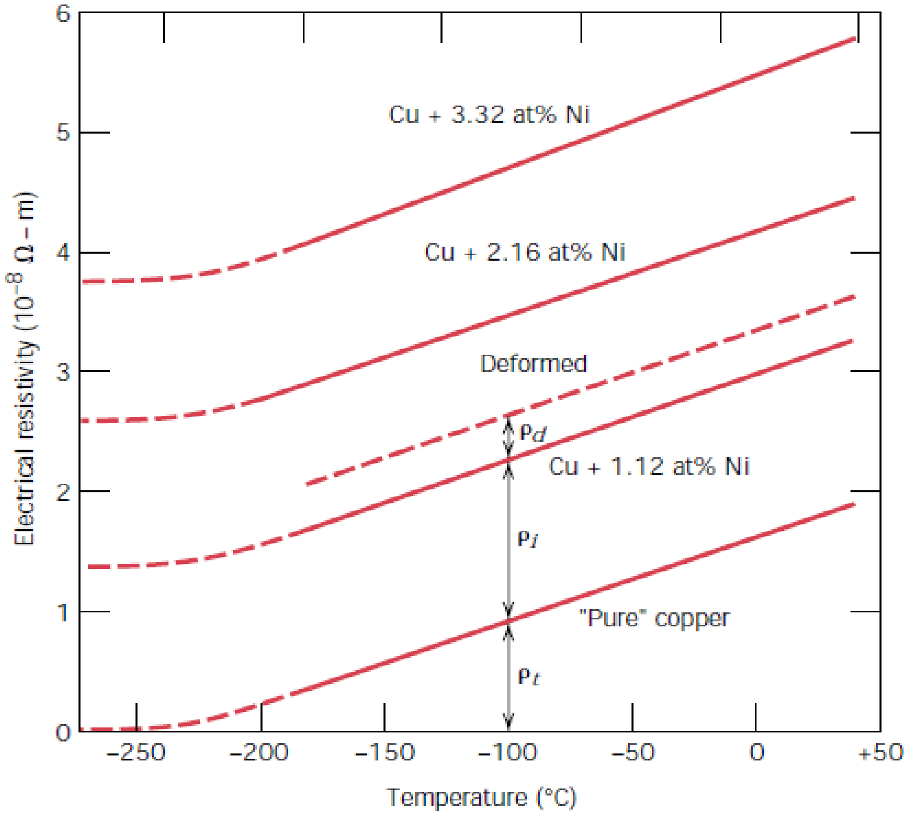

- **Increase with temperature**

Increase in thermal vibrations and other lattice irregularities (e.g., vacancies): electron-scattering centers.

- **Constant at very low temperature**

the mean free path is dominated by impurities or defects in the material

Electrical Properties of Materials

'sweet spot' R ~ **1 Ohm -1 MOhm**

2p

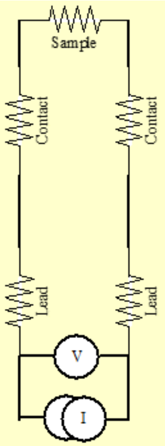

4p

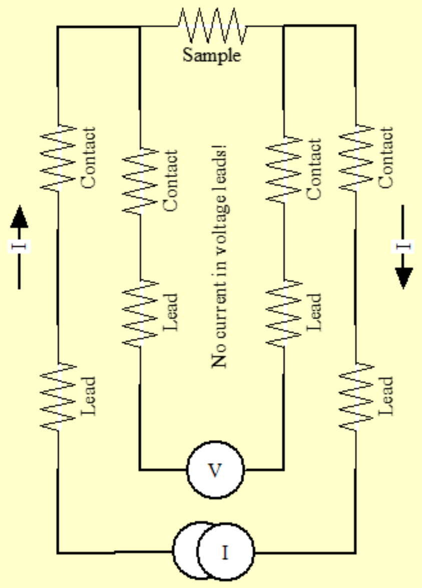

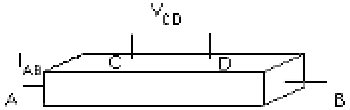

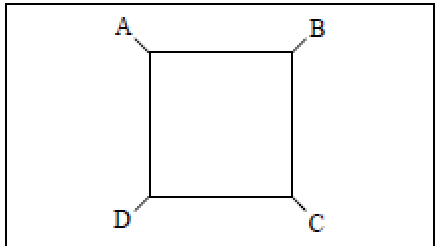

Figure 2. Typical van der Pauw Measurement

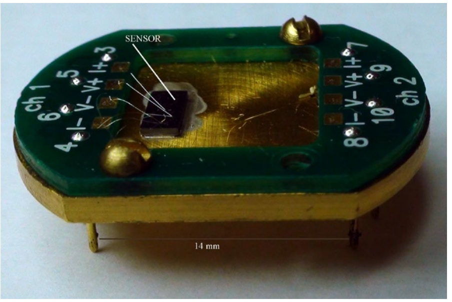

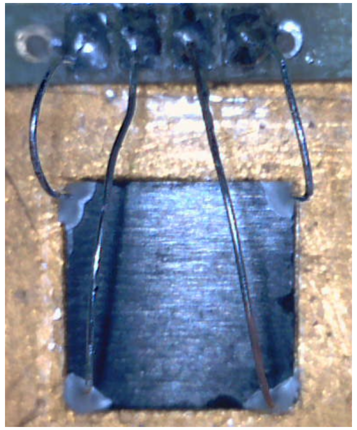

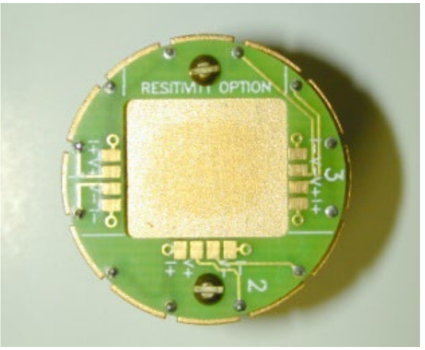

R=V/I

spring-loaded pins

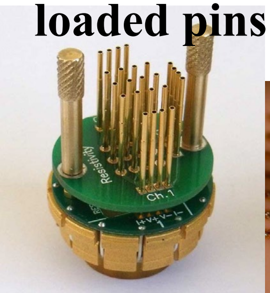

PC-RES-P

wire bonder

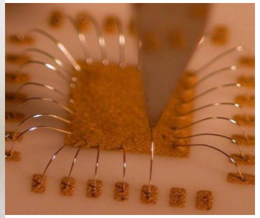

solders **Ag epoxy** **Ag paint**

Electrical Properties of Materials

Measure of the superconducting transition $T_c(T,H,I)$

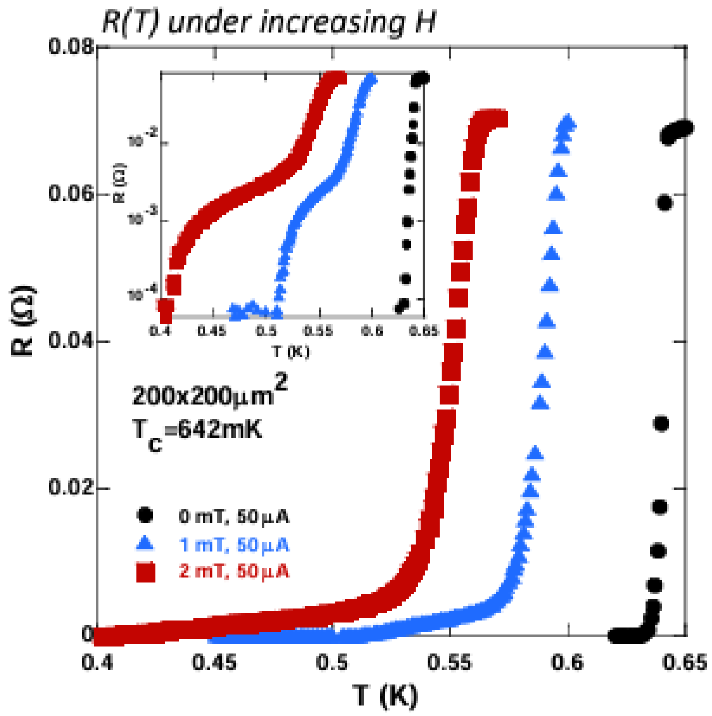

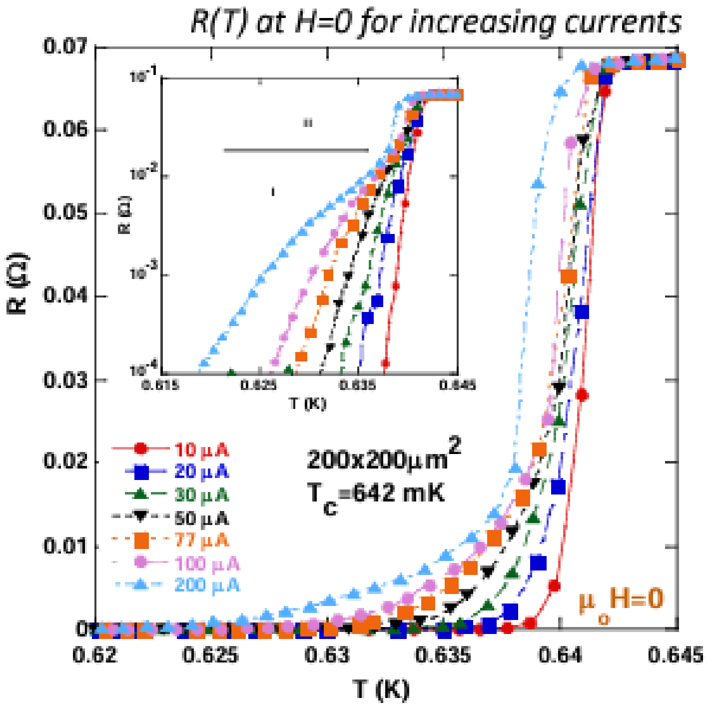

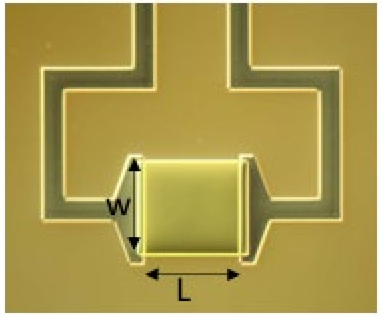

2D Mo/Au bilayers Transition Edge Sensors (TESs)

Fabrega L et al. 2019 Supercond. Sci. Technol. 32 015006

Electrical Properties of Materials: metals

$$RRR = \frac{\rho_{300K}}{\rho_{0K}}$$

RRR vary quite strongly for a single material depending on the amount of impurities and other crystallographic defects

It serves as a rough index of the purity and overall quality of a sample

Cu Residual-resistivity ratio

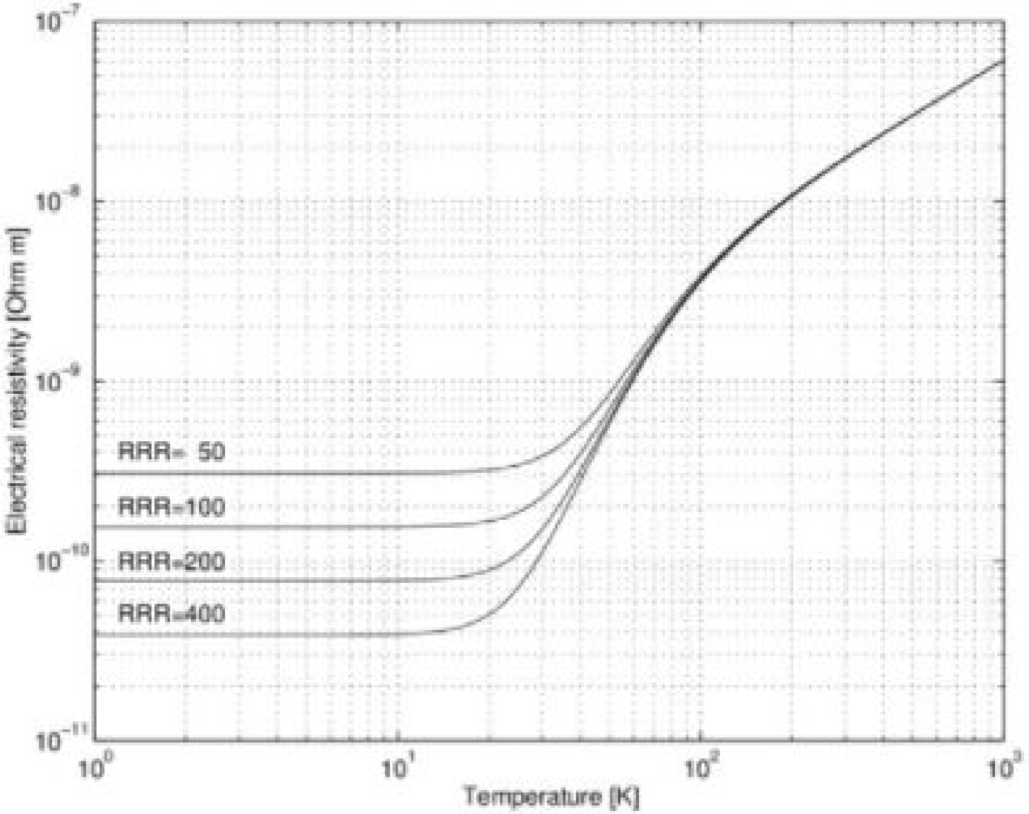

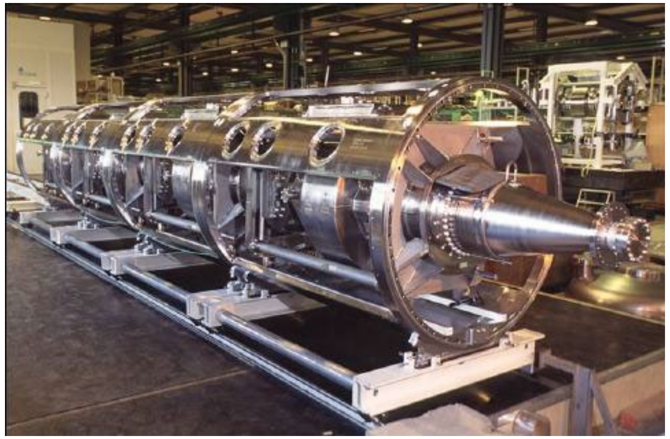

LHC RF cavities operate at 4.5 K

Pure niobium in its superconducting state (T_c = 9.2K) is used for high-quality-factor **resonant cavities for particle accelerators.**

Interstitial impurities (O, N, C, H) have major influence on the thermal conductivity of niobium, damaging cavity performance.
The total impurities content can be determined by measuring the RRR.

Thermal Properties

Temperature
Heat Management

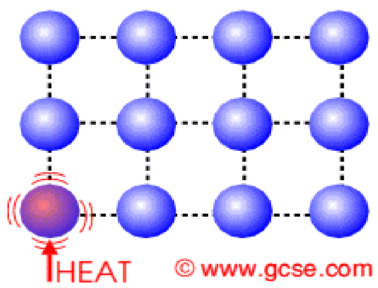

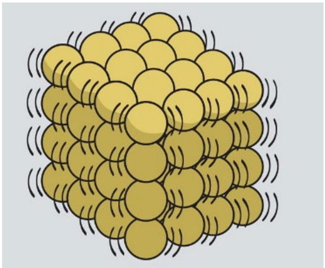

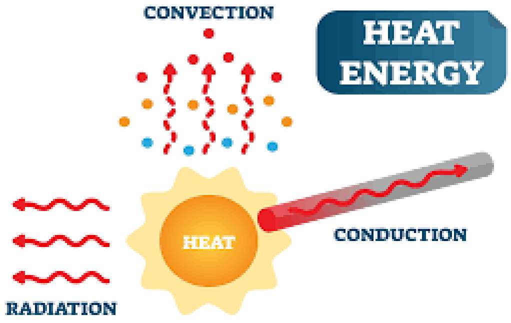

Experimental complications and constraints

- Heat Flow control
- Heat radiation
- Small Temperature differentials measurements

Heat Capacity: Specific Heat – C_P

- Information extracted, models
- Adiabatic, semiadiabatic

10^4-10^5 range

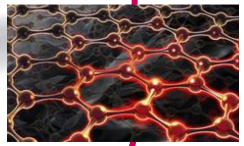

Thermal ***k***: 0.01 – 2200 – 5000 W/mK

Electrical **σ**: 10^{-20} to 10^7 $ohm^{-1}m^{-1}$

10^{27} range

Thermal Conductance, *K*: Thermal conductivity *k*

- Information extracted, models
- Steady-state, Dynamic

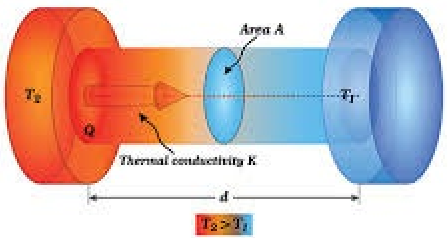

Specific Heat: Most fundamental thermodynamic property

Related to the internal energy of a system
Contains information about all the degrees of freedom

$$C = C_{ph} + C_m + C_e + C_{hf} = C_{ph} + C_m + \gamma T + \frac{\alpha}{T^2}$$

Lattice specific heat, determined by the normal modes of vibrations available to its structure

(*)

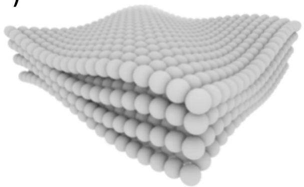

Lattice Debye Model
Solid as an isotropic continuum médium

$$C_P \cong C_V = C_{ph} = 9Nk_B \left(\frac{T}{T_D}\right)^3 \int_0^{x_D} dx \frac{x^4 e^x}{(e^x - 1)^2}$$

$x = \hbar\omega / k_B T$
$T_D = \hbar\omega_D / k_B$

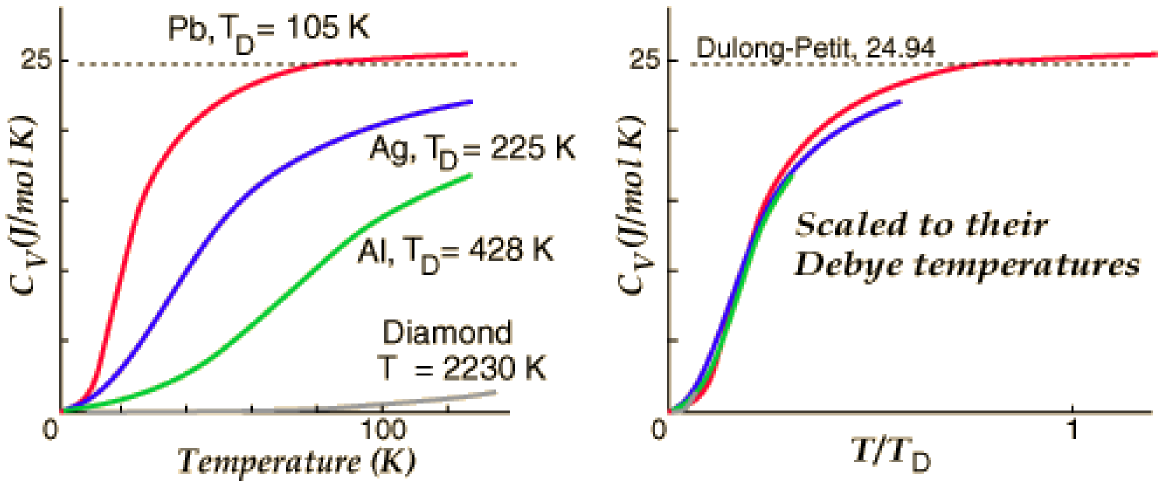

Low T, $T \ll T_D$	$C_P \cong \frac{12\pi^4}{5} NR \left(\frac{T}{T_D}\right)^3 = AT^3$
High T, $T \gg T_D$	$C_P \cong 3NR$

(*) Collective motions called phonons. *Credit: Sean Kelley/NIST*

Specific Heat: Standard Characterization

***Low T C*(T) ~ *AT*³**

First Order Transitions

C(T), C_L Characterization:

Sensible heat, Latent Heat

Debye Temperature

$\theta_D = T_D = \hbar\omega_D/k_B = \hbar\upsilon_s\,(6\pi^2 N/V)^{1/3}/k_B$

υ_s velocity of sound

Latent Heat

First Order Phase Transitions FOPT

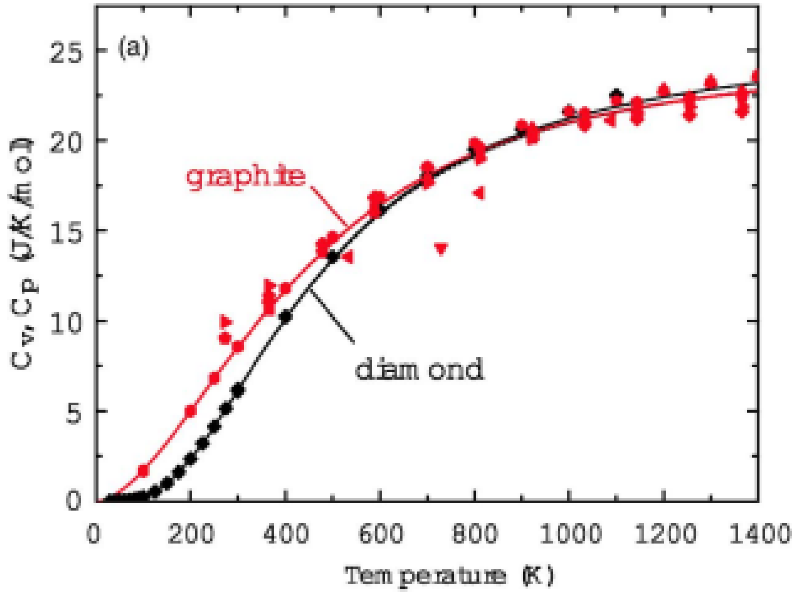

The Debye temperature θ_D is the temperature of a crystal's highest normal mode of vibration, and it correlates the elastic properties (structural rigidity), thermal expansion, thermal conductivity, and specific heat

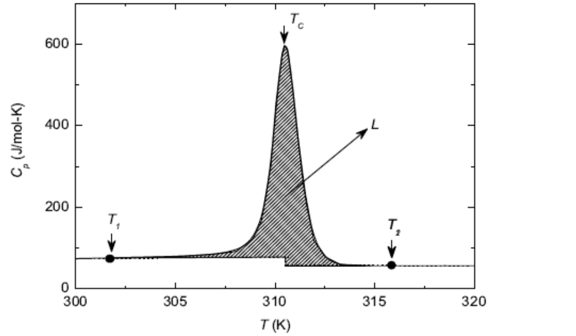

Figure 2.2: Temperature dependence of the heat capacity at zero field for $Mn_{0.997}Co_{0.003}As$. The value of shaded area indicates the latent heat associated to a FOPT. The stepped line represents the normal heat capacity.

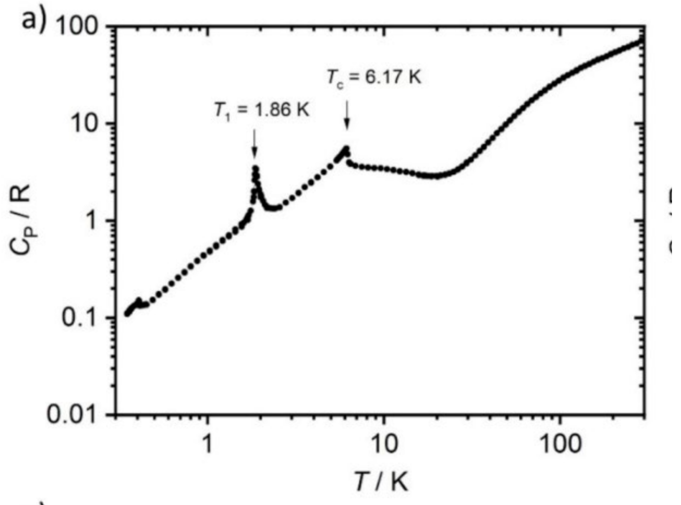

Structural Investigation into Magnetic Spin Orders of a Manganese Phosphatic Oxyhydroxide, Mn5[(PO4)2(PO3(OH))2](HOH)4
Partk et al.
Symmetry 2021, 13(9), 1688; https://doi.org/10.3390/sym13091688

Heat Capacity Techniques

- Adiabatic
- Semiadiabatic
- Ac calorimetry

$$C = C_P = \left(\frac{dQ}{dT}\right)_P \xrightarrow[Adiabatic]{} \left(\frac{\Delta Q}{\Delta T}\right)_P$$

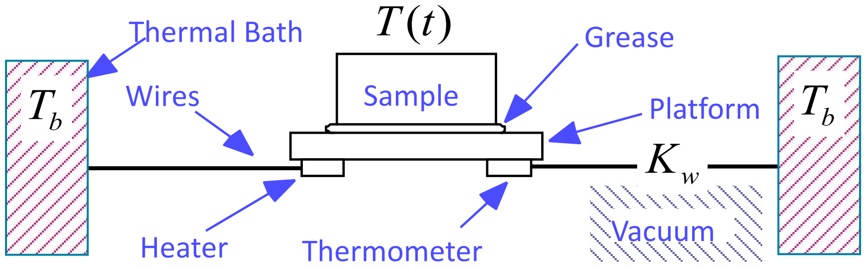

$$C_{\text{total}} \frac{dT(t)}{dt} = P(t) - K_w(T(t) - T_b)$$

Adiabatic:
P= P_0, t = t_0 pulse
$t_0 >> \tau = C/K$ stationary
C ≈ Q/ΔT

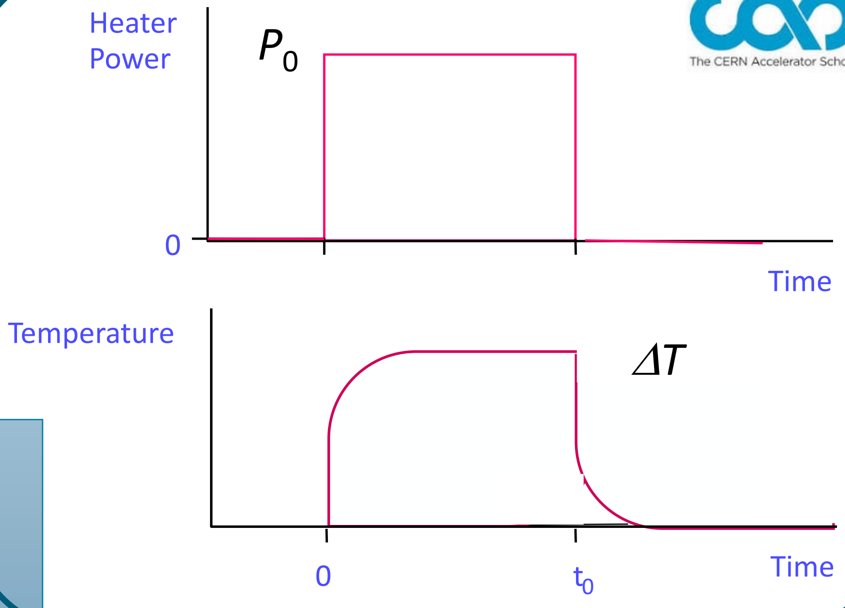

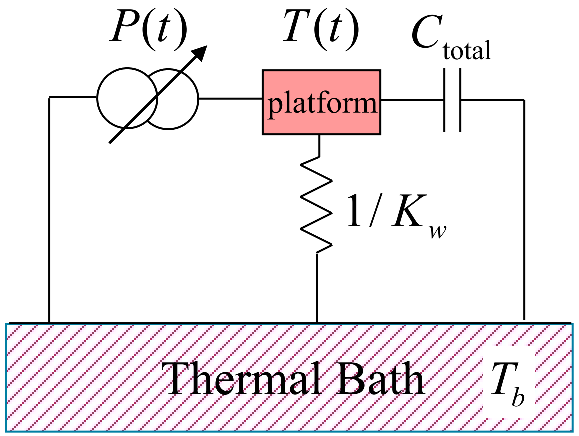

$$P(t) = \begin{cases} P_0 & (0 \le t \le t_0) \\ 0 & (t > t_0) \end{cases}$$

Semiadabatic relaxation method[1]
P= P_0, t = t_0 pulse
$t_0 = 2\tau = 2C/K$
C = τ ·K_w

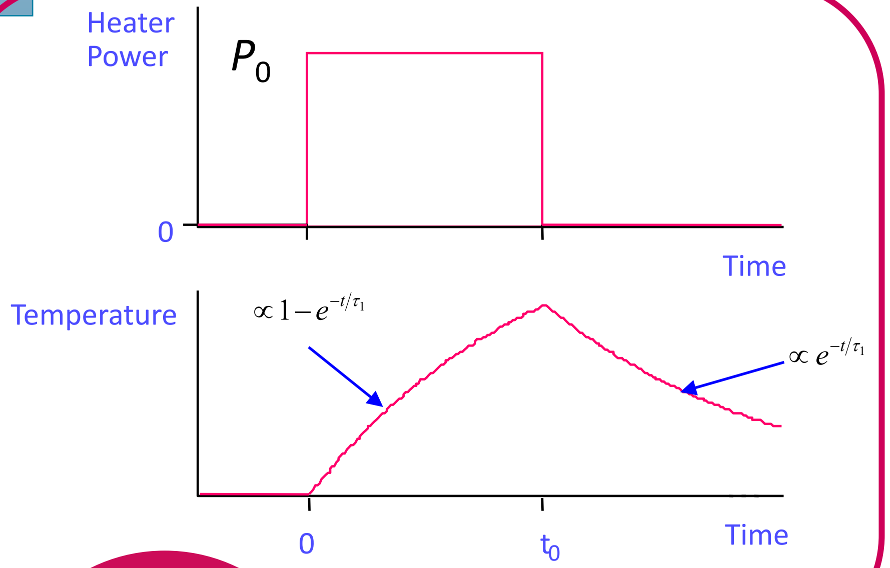

(1) Measurement of heat capacity by fitting the whole temperature response of a heat-pulse calorimeter
Jih Shang Hwang, Kai Jan Lin, and Cheng Tien
Review of Scientific Instruments 68, 94 (1997); https://doi.org/10.1063/1.1147722

Heat Capacity semi-adiabatic relaxation method

Implementation in HC option of PPMS Quantum Design(*)

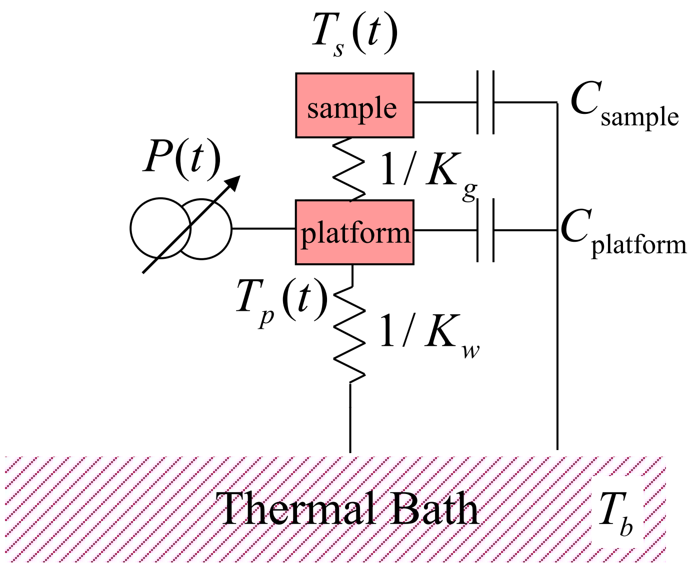

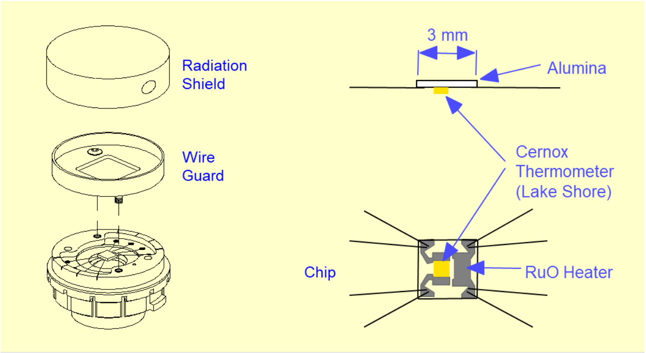

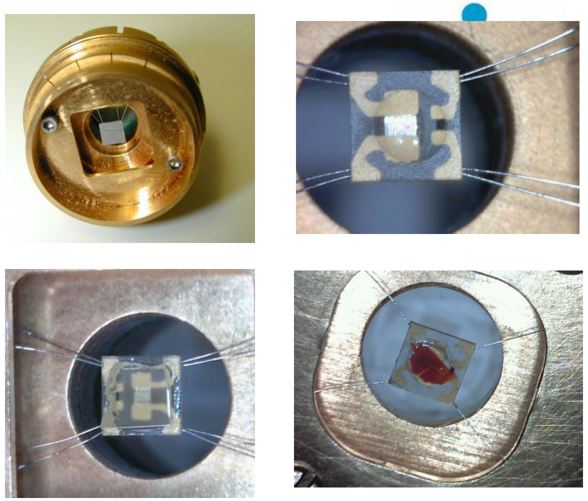

Samples: 0.1 mg – 100 mg   Solid, powder, ‘liquid’

$$C_{sample}\frac{dT_s(t)}{dt} = -K_g\left(T_s(t)-T_p(t)\right)$$

$$C_{platform}\frac{dT_p(t)}{dt} = P(t) - K_w\left(T_p(t)-T_b\right) + K_g\left(T_s(t)-T_p(t)\right)$$

unknowns

Model limitation for *C* divergence (1st order transition)

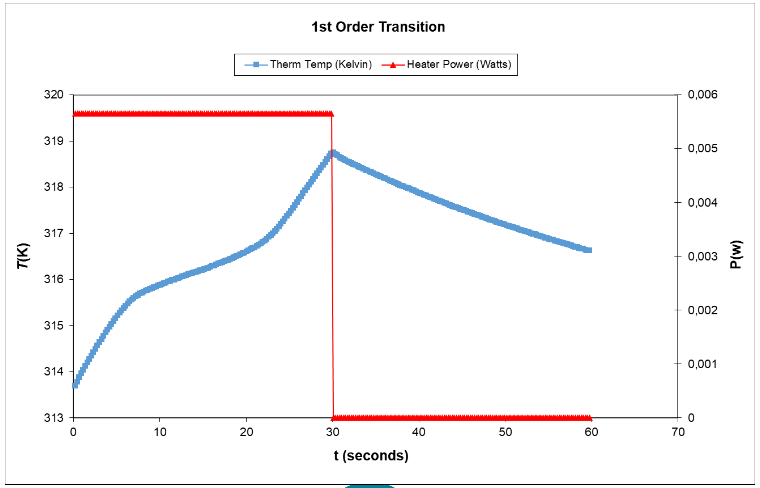

- Single pulse análisis
- Relaxation method with small ΔT steps (infinitesimal approach)

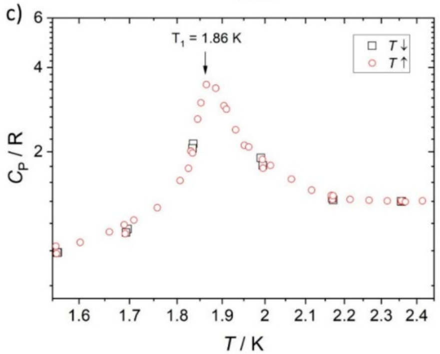

http://sai.unizar.es/medidas-fisicas-eng/hc

Critical examination of heat capacity measurements made on a Quantum Design physical property measurement system, J.C. Lashley et al. Cryogenics, Volume 43, Issue 6, 2003,Pages 369-378, https://doi.org/10.1016/S0011-2275(03)00092-4.

Thermal Conductivity

- Thermal conductance: ratio of **steady-state** heat flow to temperature difference

$$K = \dot{Q}_{th} / \Delta T \ \text{W/K}$$

$$\boldsymbol{\kappa} = \boldsymbol{K}\,(\boldsymbol{L/A}) \ \text{W/m·K}$$

Information on the scattering of electrons and phonons

$\kappa = 1/3\ C\langle v\rangle\langle l\rangle$

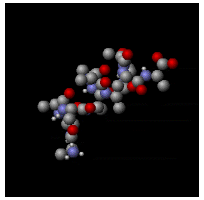

➢ Sources of phonon scattering:
Defects, interactions, interfaces

➢ Heat transfer at the nanoscale
Size dependent termal conductivity

➢ Low-energy phonon structure

INS + Calculations ⇔ Experimental k

Study of processes taking place in thermal conduction

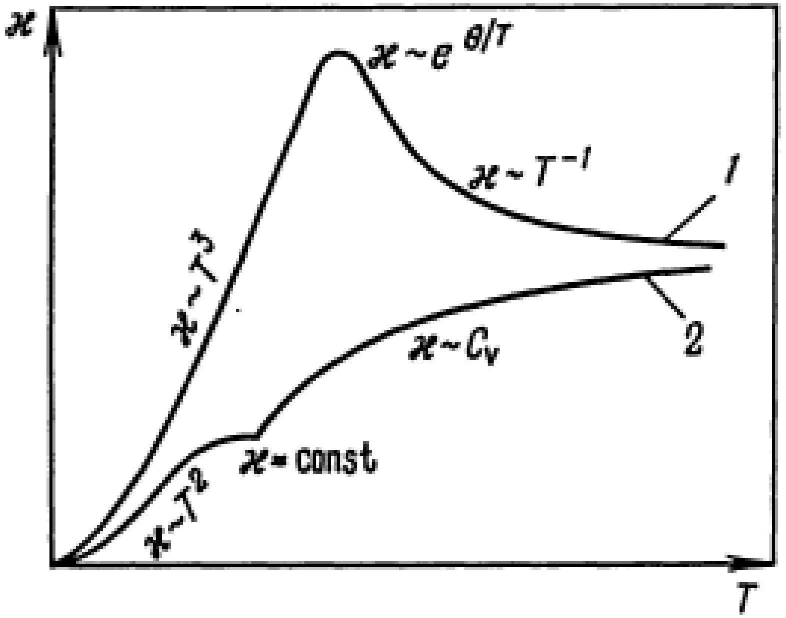

Schematic drawing of the temperature dependence of the conductivity of crystalline (1) and amorphous (2) dielectric solids

Yuli K. Godovsky. Thermophysical Properties of Polymers. Springer-Verlag 1992
DOI 10.1007/978-3-642-51670-2

Amorphous solids
Low *T* **$k \propto T^2$**

Thermal Conductivity Techniques

1-heater 2-thermometers method
Thermal Circuit

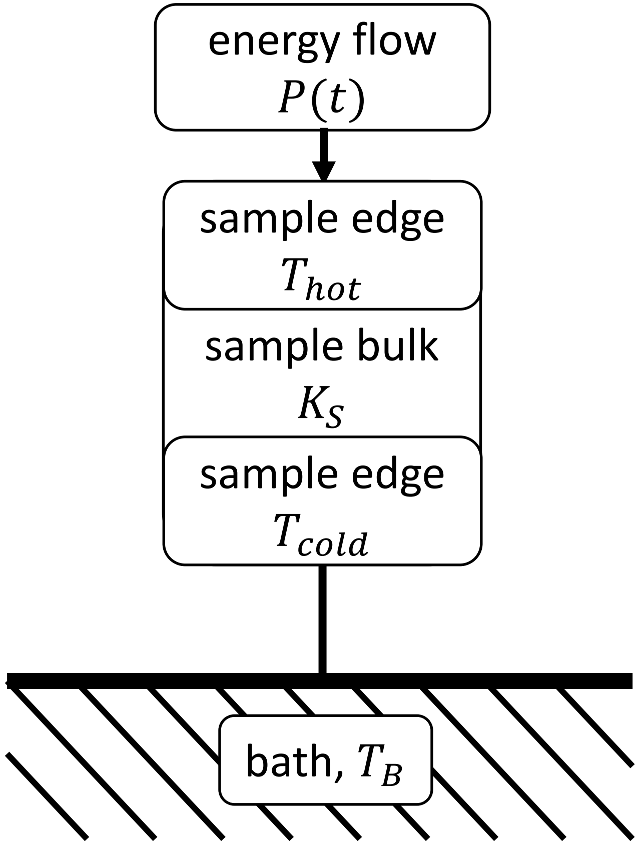

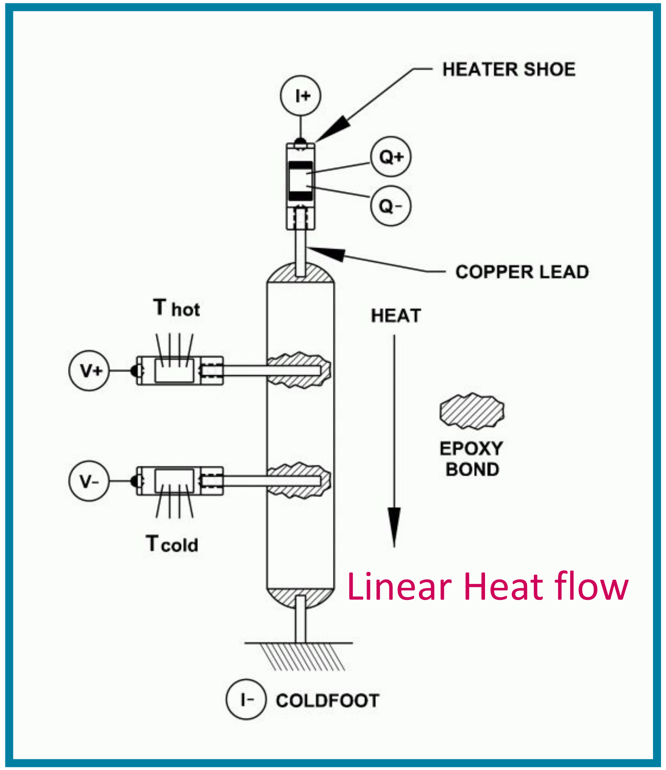

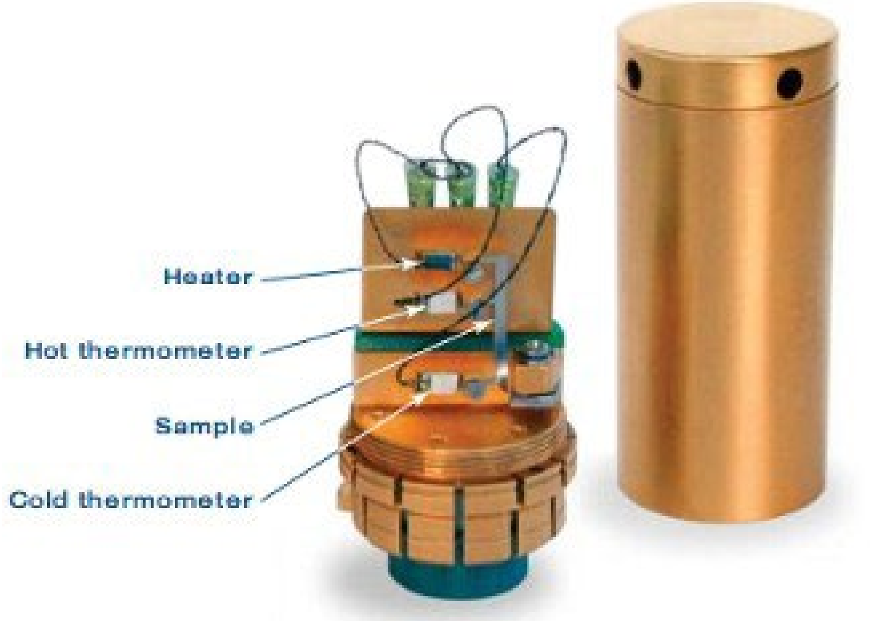

➤ *Thermal Transport sample puck with radiation shield*

Thermal Conductivity Techniques: comercial TTO from PPMS (QD)

- Temperature: 1.9 K - 390 K

- **High vacuum (~10^{-4} torr)**

- Magnetic Field

0 a ± 140 kOe for T > 20 K
0 a 1 kOe for T < 20 K

Lead Configuration:
- 2-Probe
- 4- Probe

- **Range of *k*** and sample geometries

10-150 W/mK (Needle: 10x1x1 mm³)
2-30 W/mK (Brick: 8x2x2 mm³)
0.1-1.5 W/mK (Pill: 3x5x5 mm³)

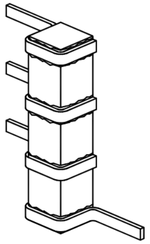

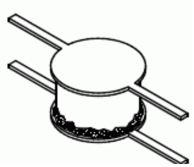

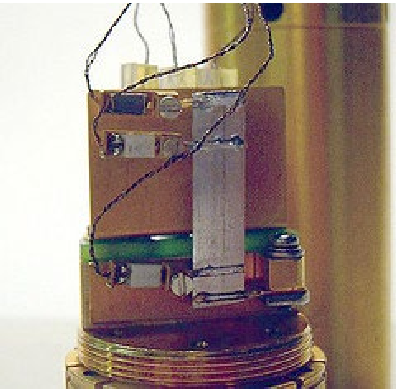

Carbon fiber/epoxy composites

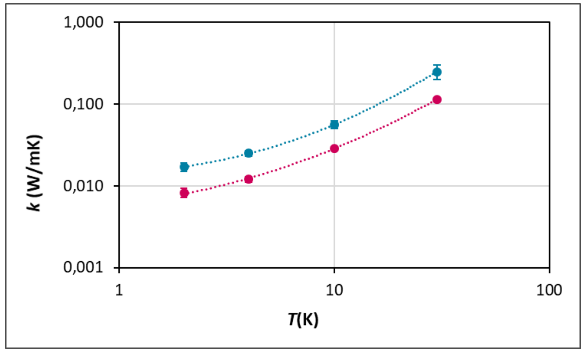

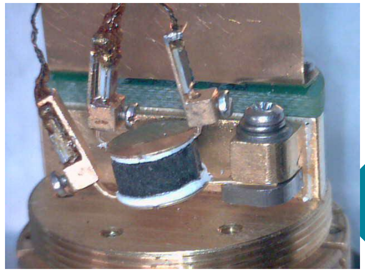

Limitations:
High *k*: Maximum heating power 50 mW
Low *k* : Measurement time

http://sai.unizar.es/medidas-fisicas-eng/tto

Thermal Conductivity TTO

Steady-state solution

Only for very high k samples
k > 200 W/mK

$$\Delta T(t) = \frac{P_0}{K_s}\left[1 - \left(\frac{\tau_1 e^{-t/\tau_1} - \tau_2 e^{-t/\tau_2}}{\tau_1 - \tau_2}\right)\right]$$

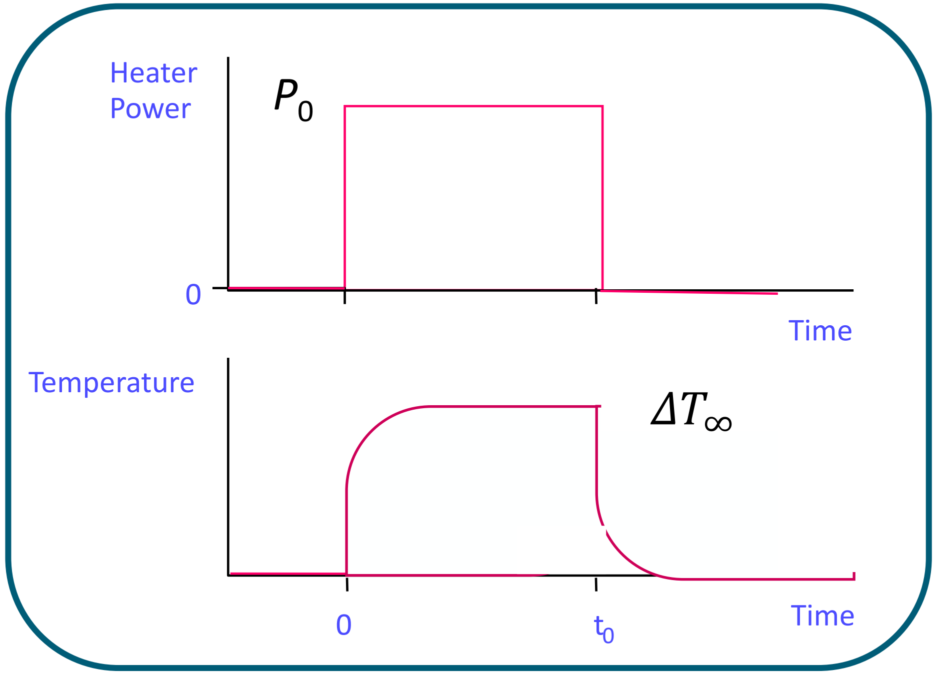

In the asymptotic limit,

$$\Delta T(t \to \infty) = \boldsymbol{\Delta T_\infty} = \boldsymbol{P_0 / K_s}$$

P_0 is the power supplied to the sample, nominally $P_{\mathrm{htr}} = I^2 R_{\mathrm{htr}}$

Radiated Power: $P_{\mathrm{rad}} = \sigma_T \times \left(\frac{S}{2}\right) \times \epsilon \times (T_{hot}^4 - T_{cold}^4)$

σ_T is the Stefan-Boltzmann constant

S and ϵ are the surface area and infrared emissivity of the sample, respectively

$$K_S \equiv \left((P_{\mathrm{htr}} - P_{\mathrm{rad}}) / \Delta T_\infty \right) - K_{\mathrm{shoes}}$$

Finally, geometric factors can be applied to express this as the intrinsic thermal *conductivity*:

$$\boldsymbol{\kappa_S = \frac{L}{A}\left[\left((P_{htr} - P_{rad}) / \Delta T_\infty\right) - K_{shoes}\right]}$$

Thermal Conductivity TTO

Dynamic solution

$$M(\tau_1,\tau_2\,;t) = 1 - \frac{\tau_1\, e^{-t/\tau_1} - \tau_2\, e^{-t/\tau_2}}{\tau_1 - \tau_2} \qquad \text{(heating)}$$

Long diffusion times
$\tau_1 \approx C_{sample}/K_{sample}$ → Model of Thermal History

$$\Delta T(\Delta T_\infty, \tau_1, \tau_2\,; t) = \Delta T_\infty \times [M(t-t_0) + P_{-1}M(t-t_{-1}) + P_{-2}M(t-t_{-2})]$$

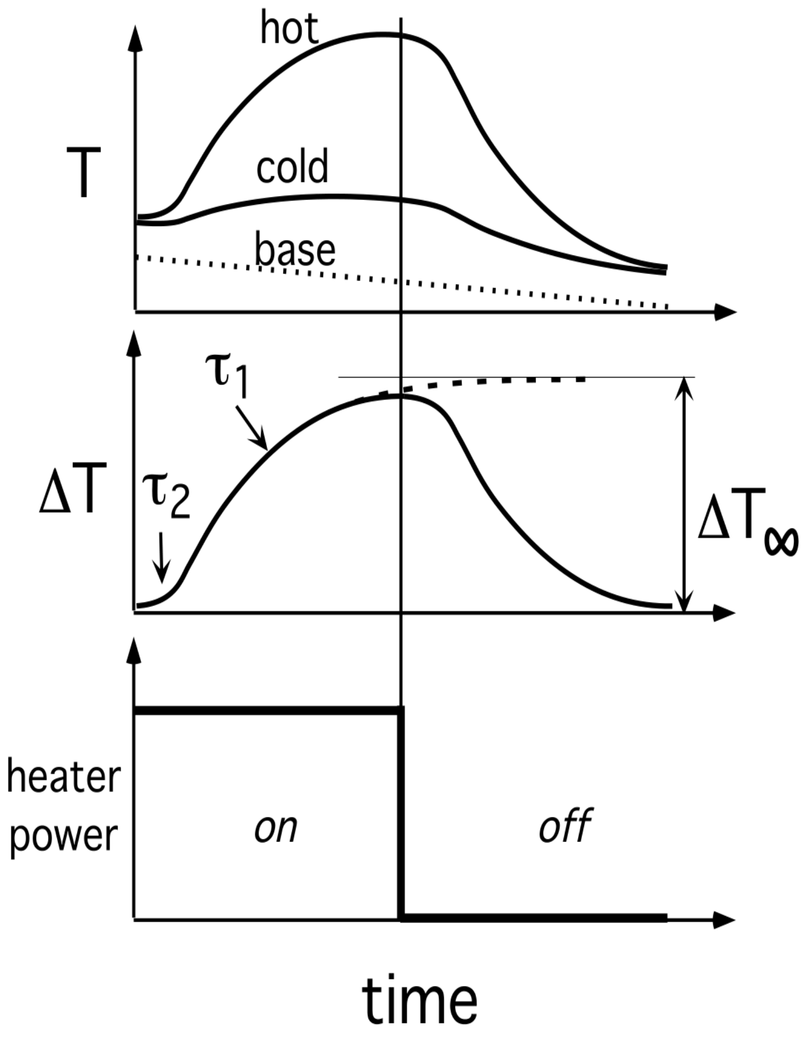

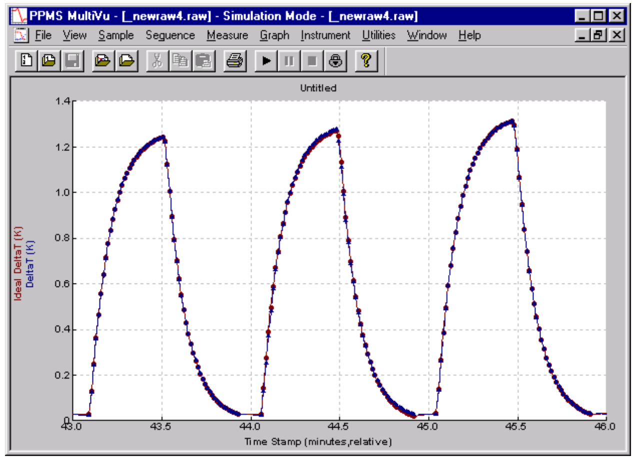

Thermal Properties of materials: NITRONIC 50

Physical Properties of Nitronic 50 ITER

Collaboration University of Zaragoza - Engineering Department at CERN. A. Arauzo and Stefano Sgobba.

Nitronic® 50 High Strength
high N and Mo austenitic stainless steel
Non-magnetic, with low μ even at cryogenic T's.

ITER project (International Thermonuclear Experimental Reactor). Central solenoid compression structure

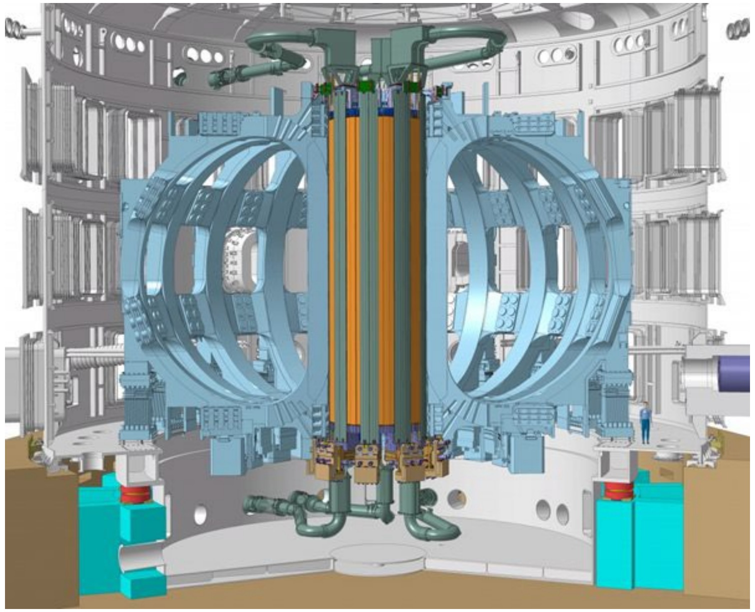

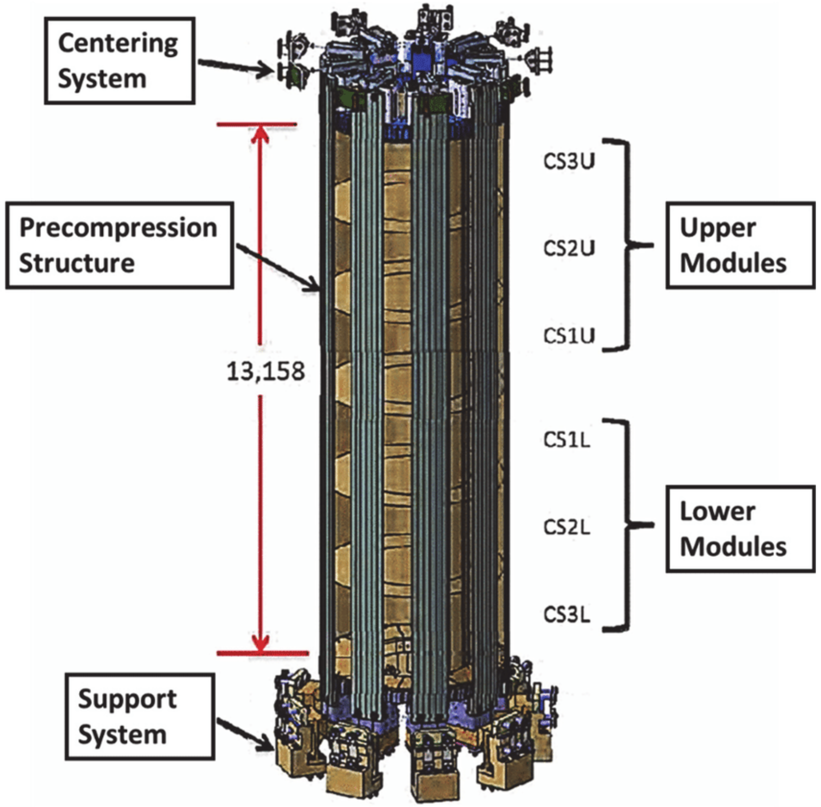

Central solenoid: the strongest of all ITER magnets
Maximum field of 13 T

https://www.iter.org/newsline/-/3233#:~:text=The%20ITER%20central%20solenoid%20is,a%20pre%2Dcompression%20support%20structure.

S. Sgobba, S. A. E. Langeslag, A. Arauzo, P. Roussel and P. Libeyre, "Physical Properties of a High-Strength Austenitic Stainless Steel for the Precompression Structure of the ITER Central Solenoid," in IEEE Transactions on Applied Superconductivity, vol. 26, no. 4, pp. 1-4, June 2016, Art no. 7000104, doi: 10.1109/TASC.2016.2535388.

Thermal Properties of materials: NITRONIC 50

The tie plates **operating at 4 K** can be manufactured:

a) from single forgings ("singlepiece forging" tie plate), involving blanks of more than 15 m length
b) from shorter forgings welded together

We have studied samples belonging to two different series in three different positions:

Single Piece Forged, SPF:

- SPF-TOP
- SPF-MIDDLE
- SPF-BOTTOM

Welded Solution, WS:

- WS-TOP
- WS-MIDDLE
- WS-BOTTOM

Thermal Properties of materials: NITRONIC 50

Physical characterization comprises the following measurements:

- Measurements of Thermal Conductivity and Electrical Resistivity between 293K and 4K.
- Measurements of Specific Heat between 293K and 4K.
- Measurements of Magnetization and Magnetic Permeability 293K - 4K at *H* = 7950 A/m (H=100 Oe).
- Hysteresis cycle at 295K and 4.2K up to 7162 kA/m (*H*=90000 Oe).

Thermal conductivity and specific heat capacity are significant in predicting the quench behavior and cooling process of the large-scale superconducting magnet.

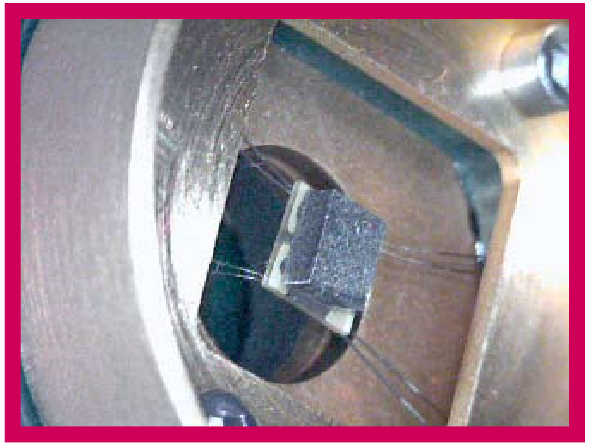

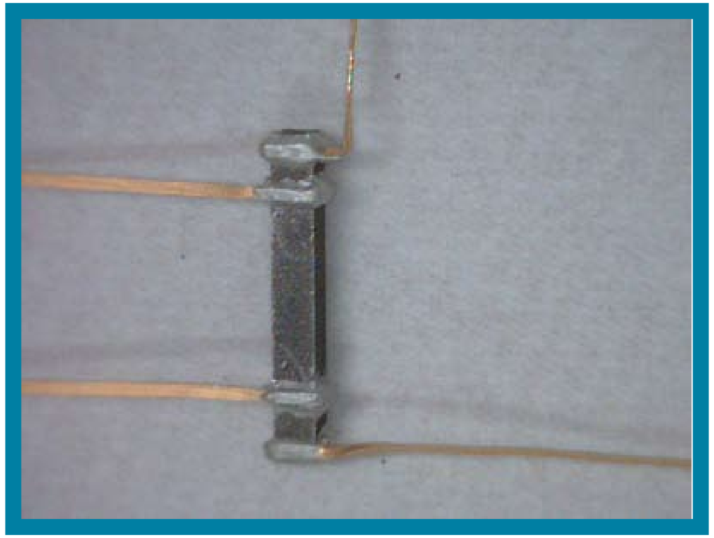

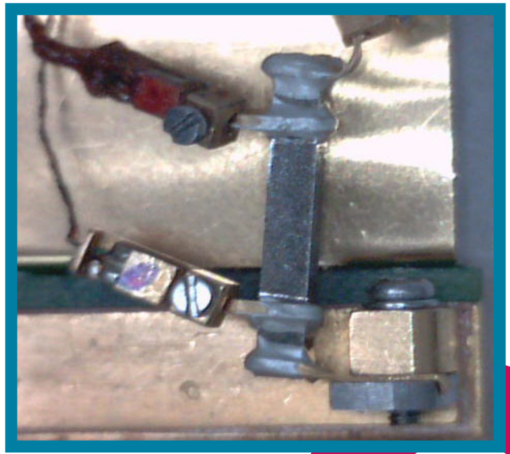

Thermal Properties of materials: NITRONIC 50

Heat Capacity: **specific heat $c_p(T)$**

Physical properties of NITRONIC 50®
RT Thermal capacity, c_p: 0.5 kJ • kg^{-1} • K^{-1}

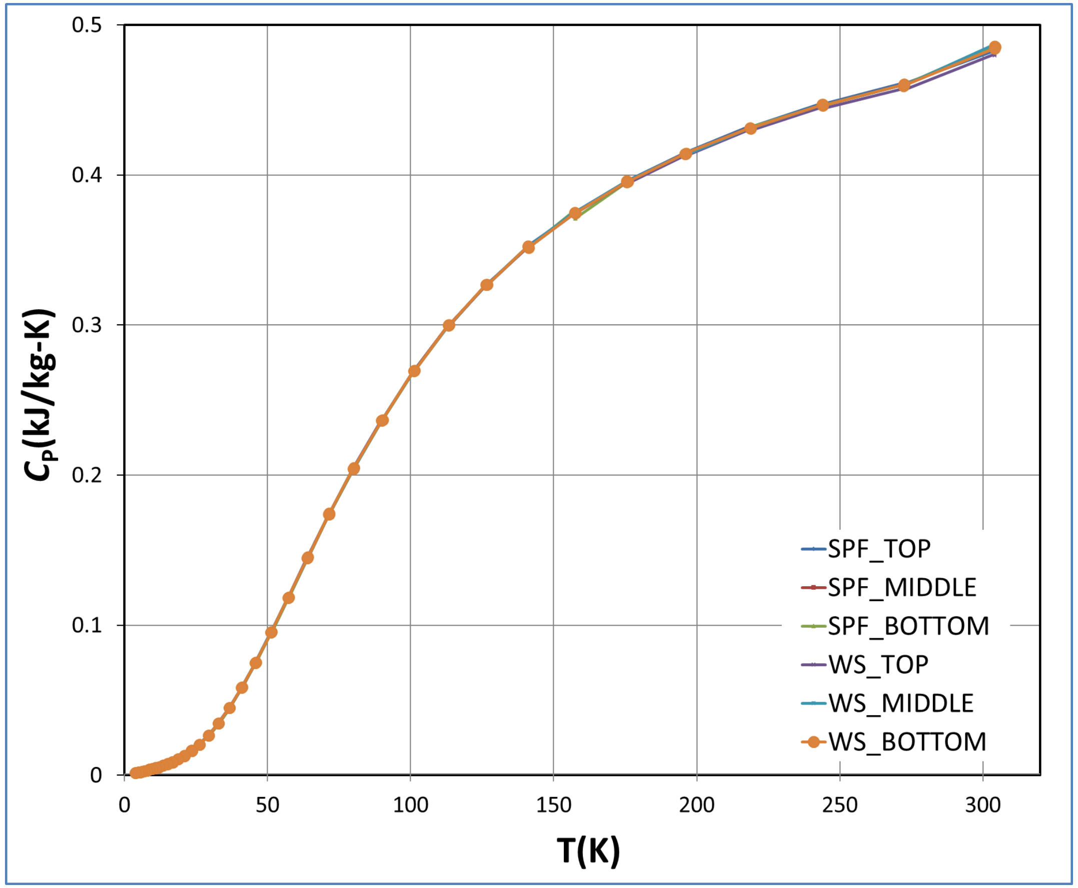

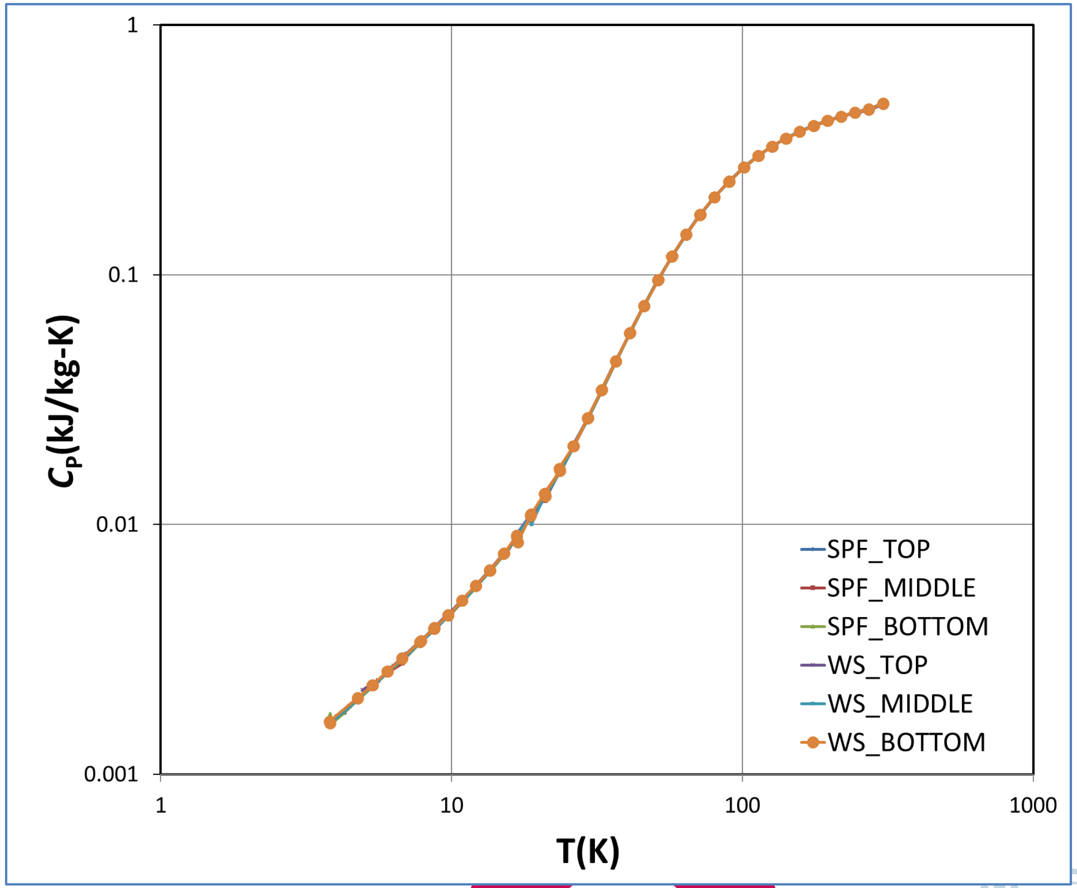

Thermal Properties of materials: NITRONIC 50

Thermal Conductivity: **k(*T*)**

Physical properties of NITRONIC 50®
Thermal conductivity, k: 15 W • m^{-1} • K^{-1}

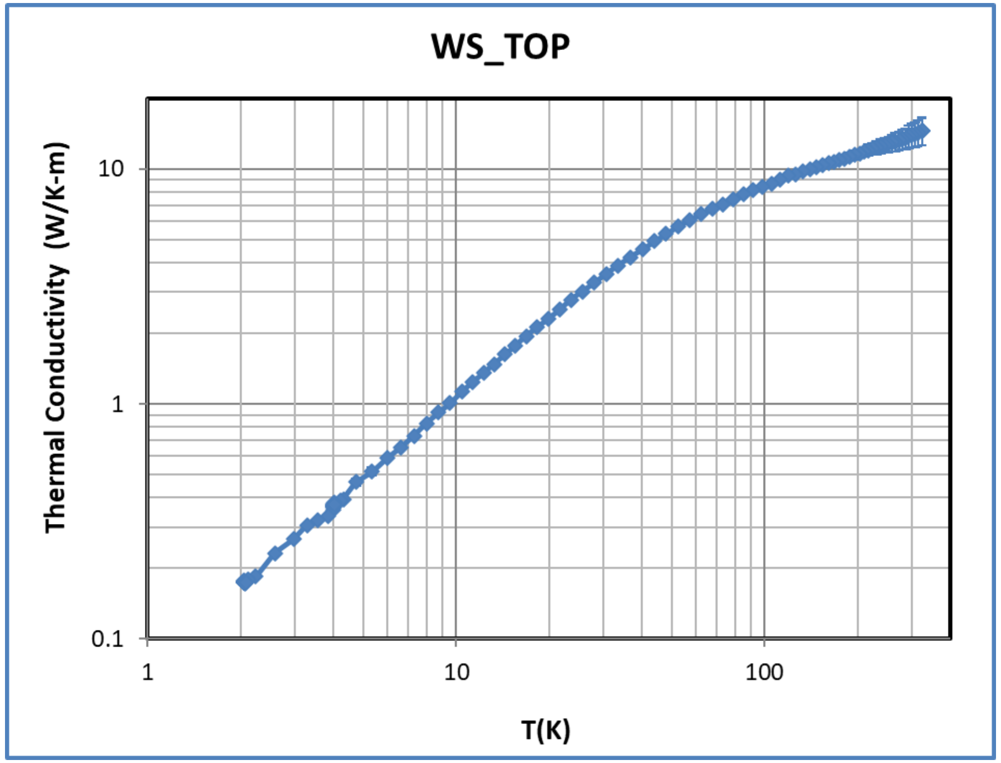

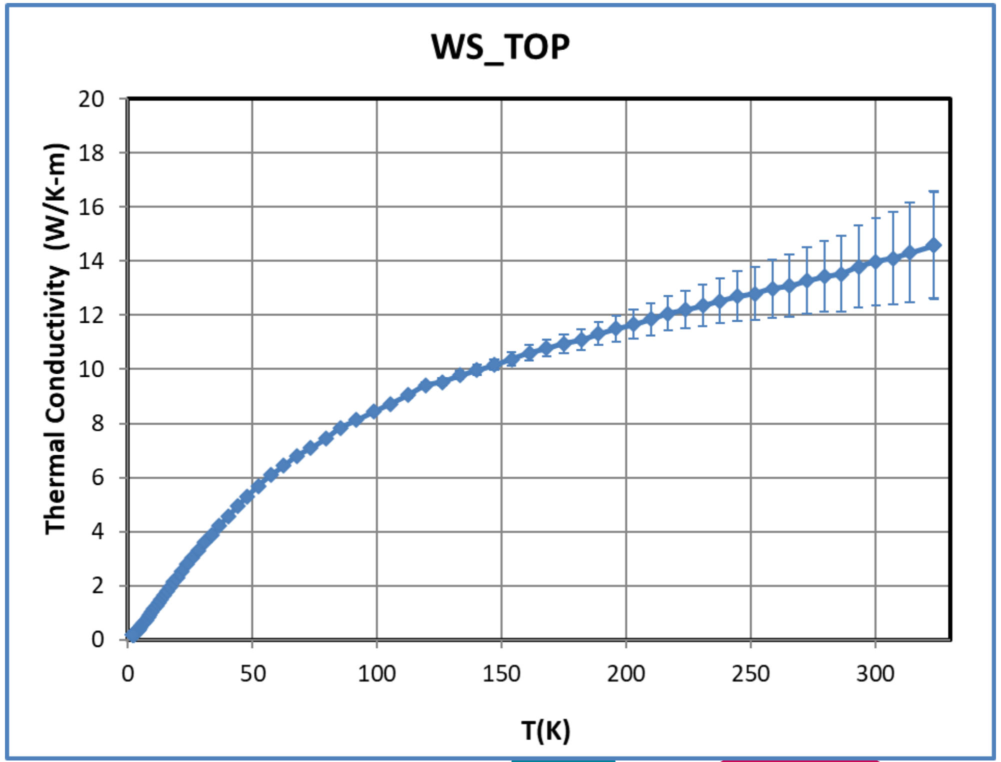

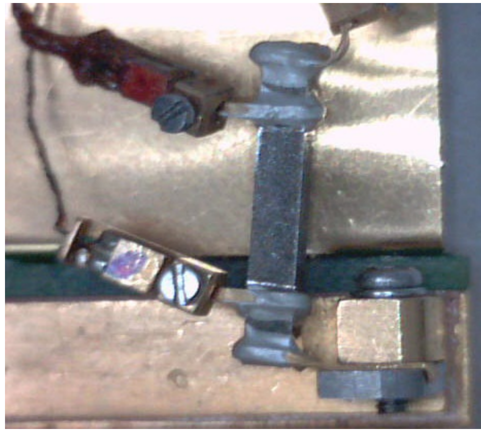

Thermal Properties of materials: NITRONIC 50

Electrical Resistivity: ρ(*T*)

Super Alloy Nitronic 50

Carbon	0.06 max
Chromium	20.5 - 23.5
Iron	Balance
Manganese	4 - 6
Molybdenum	1.5 - 3
Nickel	11.5 - 13.5
Niobium	0.1 - 0.3
Nitrogen	0.2 - 0.4
Phosphorus	0.04 max
Silicon	1 max
Sulphur	0.03 max
Vanadium	0.1 - 0.3

Physical properties of NITRONIC 50®
Electrical Resistivity, 21 °C 82 µΩ•cm

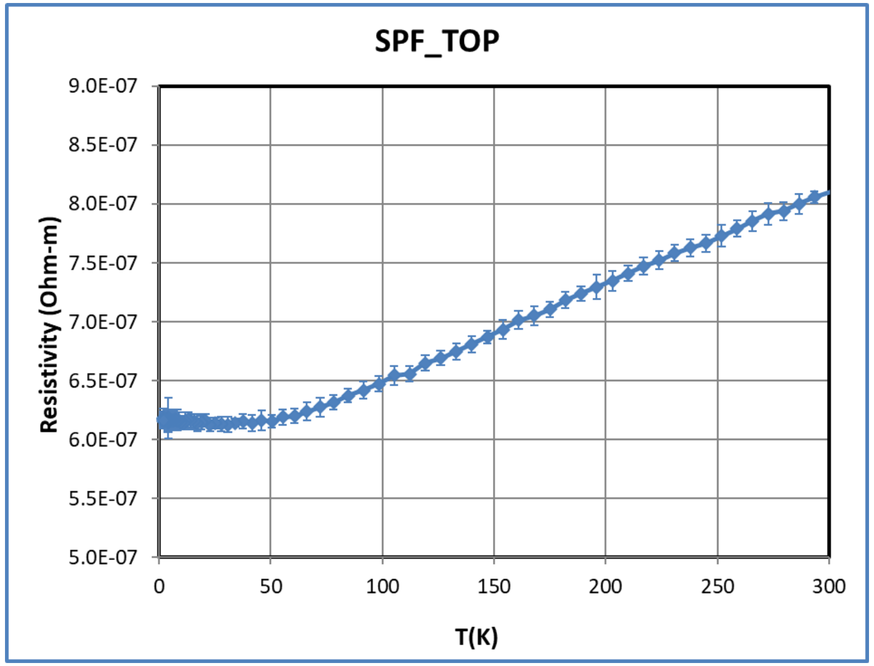

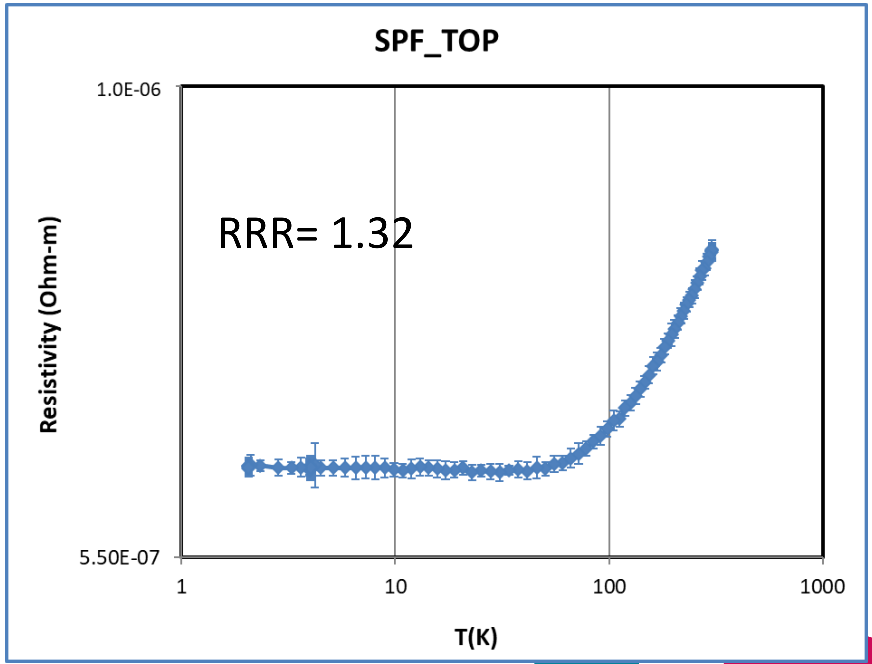

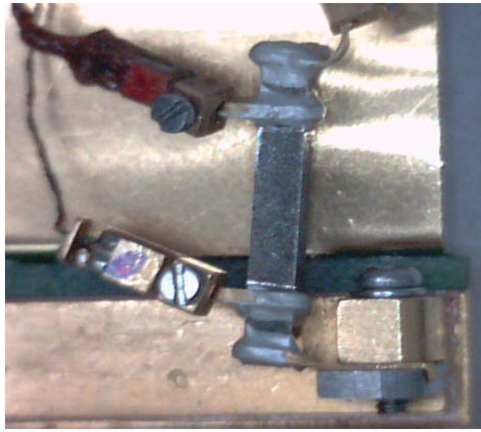

Magnetic Properties of Materials

Fundamentals

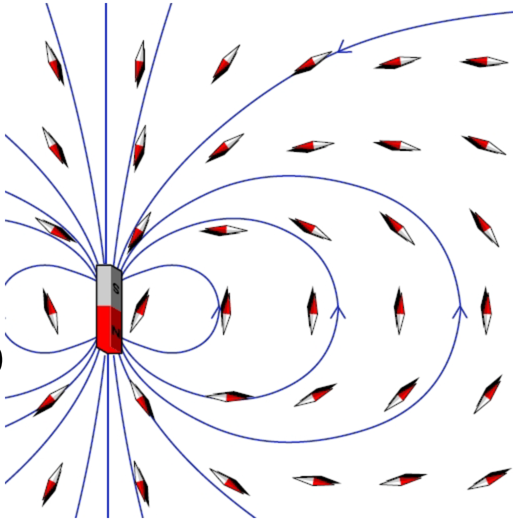

- Every material is magnetic: shows a kind of magnetic behavio

Commonly: magnetic = magnet

- A magnetometer measures the magnetic moment, the amount of magnetism in a sample.
- By studying the variation of the magnetization with temperature or the magnetic field intensity we may determine the type of magnetism of a material.
  - $M(H)$, $M(T)$

Universidad Zaragoza

Magnetic Properties of Materials

- Characteristic Magnitudes
  - Magnetic Field, H [A/m]
  - Magnetization, M [A/m] → $M = \chi H$
  - Flux density, B[T] → $B = \mu H$
  - Susceptibility, χ
  - Permeability, μ, $\mu_r = \mu/\mu_0$

Related by:

$$B = \mu_0 H + \mu_0 M = \mu_0 (1 + \chi) H = \mu H$$
$$\mu = \mu_0 (1 + \chi)$$

Magnetization, $M(H,T)$
Static magnetic properties

Types of magnetic behavior

- Diamagnetic
- Paramagnetic
- Magnetic order
  - Ferromagnetics
  - Antiferromagnetics
  - Ferrimagnetics
- Superconductors
- Superparamagnetism (NP's)

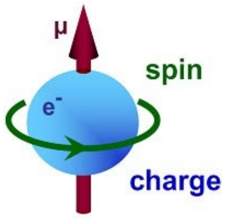

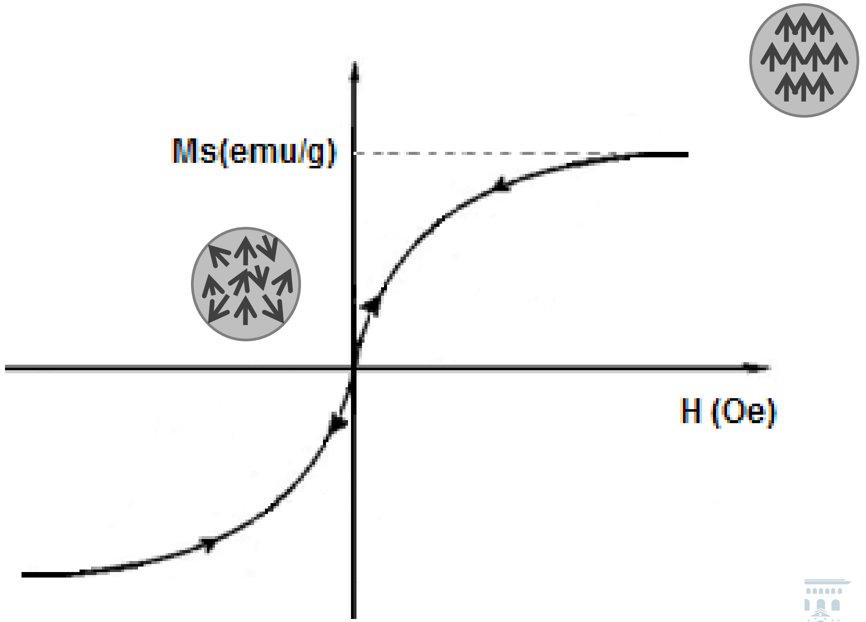

Magnetic Properties of Materials

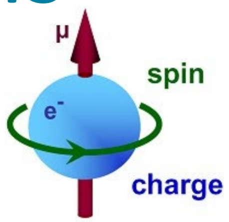

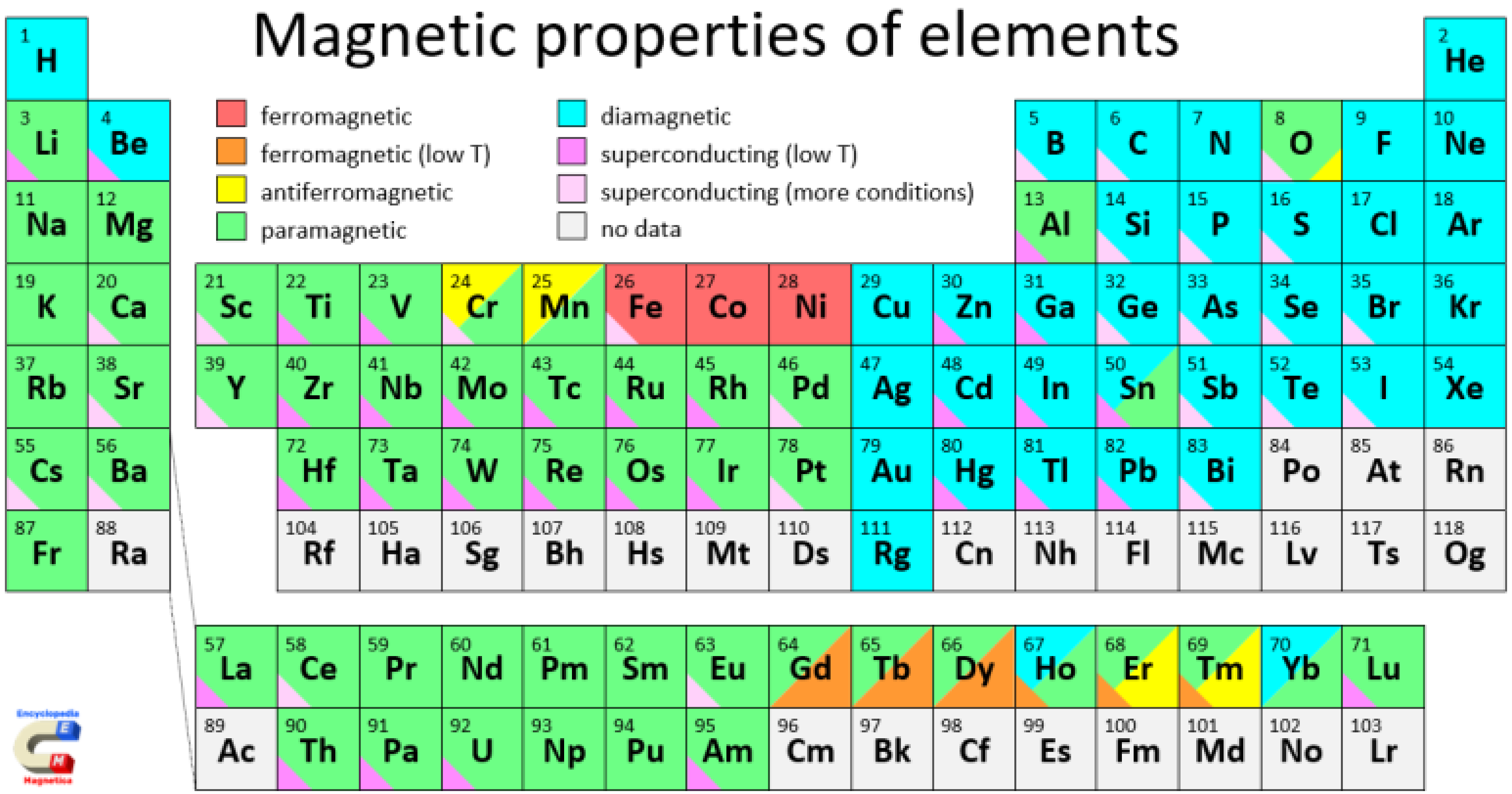

Paramagnetic Ions

Table 4.7. The 3*d* ions. m_{eff} is in units of μ_B

$3d^n$		S	L	J	g	$m_{eff} = g\sqrt{J(J+1)}$	$m_{eff} = g\sqrt{S(S+1)}$	m_{eff}^{exp}
1	Ti^{3+}, V^{4+}	$\frac{1}{2}$	2	$\frac{3}{2}$	$\frac{4}{5}$	1.55	1.73	1.7
2	Ti^{2+}, V^{3+}	1	3	2	$\frac{2}{3}$	1.63	2.83	2.8
3	V^{2+}, Cr^{3+}	$\frac{3}{2}$	3	$\frac{3}{2}$	$\frac{2}{5}$	0.78	3.87	3.8
4	Cr^{2+}, Mn^{3+}	2	2	0			4.90	4.9
5	Mn^{2+}, Fe^{3+}	$\frac{5}{2}$	0	$\frac{5}{2}$	2	5.92	5.92	5.9
6	Fe^{2+}, Co^{3+}	2	2	4	$\frac{3}{2}$	6.71	4.90	5.4
7	Co^{2+}, Ni^{3+}	$\frac{3}{2}$	3	$\frac{9}{2}$	$\frac{4}{3}$	6.63	3.87	4.8
8	Ni^{2+}	1	3	4	$\frac{5}{4}$	5.59	2.83	3.2
9	Cu^{2+}	$\frac{1}{2}$	2	$\frac{5}{2}$	$\frac{6}{5}$	3.55	1.73	1.9

Table 4.6. The 4*f* ions. The paramagnetic moment m_{eff} and the saturation moment m_0 are in units of μ_B

$4f^n$		S	L	J	g	$m_0 = gJ$	$m_{eff} = g\sqrt{J(J+1)}$	m_{eff}^{exp}
1	Ce^{3+}	$\frac{1}{2}$	3	$\frac{5}{2}$	$\frac{6}{7}$	2.14	2.54	2.5
2	Pr^{3+}	1	5	4	$\frac{4}{5}$	3.20	3.58	3.5
3	Nd^{3+}	$\frac{3}{2}$	6	$\frac{9}{2}$	$\frac{8}{11}$	3.27	3.52	3.4
4	Pm^{3+}	2	6	4	$\frac{3}{5}$	2.40	2.68	
5	Sm^{3+}	$\frac{5}{2}$	5	$\frac{5}{2}$	$\frac{2}{7}$	0.71	0.85	1.7
6	Eu^{3+}	3	3	0	0	0	0	3.4
7	Gd^{3+}	$\frac{7}{2}$	0	$\frac{7}{2}$	2	7.0	7.94	8.9
8	Tb^{3+}	3	3	6	$\frac{3}{2}$	9.0	9.72	9.8
9	Dy^{3+}	$\frac{5}{2}$	5	$\frac{15}{2}$	$\frac{4}{3}$	10.0	10.65	10.6
10	Ho^{3+}	2	6	8	$\frac{5}{4}$	10.0	10.61	10.4
11	Er^{3+}	$\frac{3}{2}$	6	$\frac{15}{2}$	$\frac{6}{5}$	9.0	9.58	9.5
12	Tm^{3+}	1	5	6	$\frac{7}{6}$	7.0	7.56	7.6
13	Yb^{3+}	$\frac{1}{2}$	3	$\frac{7}{2}$	$\frac{8}{7}$	4.0	4.53	4.5

Magnetic Properties of Materials

Ferromagnetism

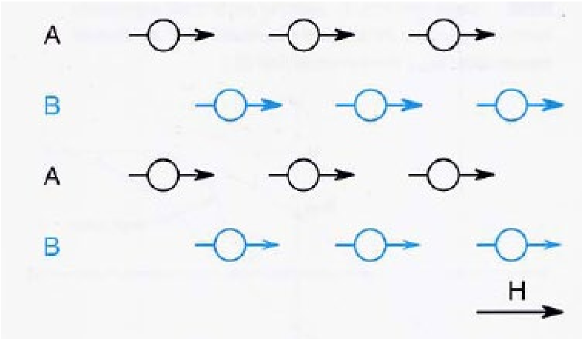

- FM is the strongest magnetism in materials
- Characteristic curves $M(H)$ and $M(T)$
  - $M(H)$ is not lineal and irreversible-> Hysteresis
  - Characteristic Parameters, M_S, M_{rem}, H_c, μ

M_S Intrinsic Parameter

$M_S(0) = N\mu_B g_J J$

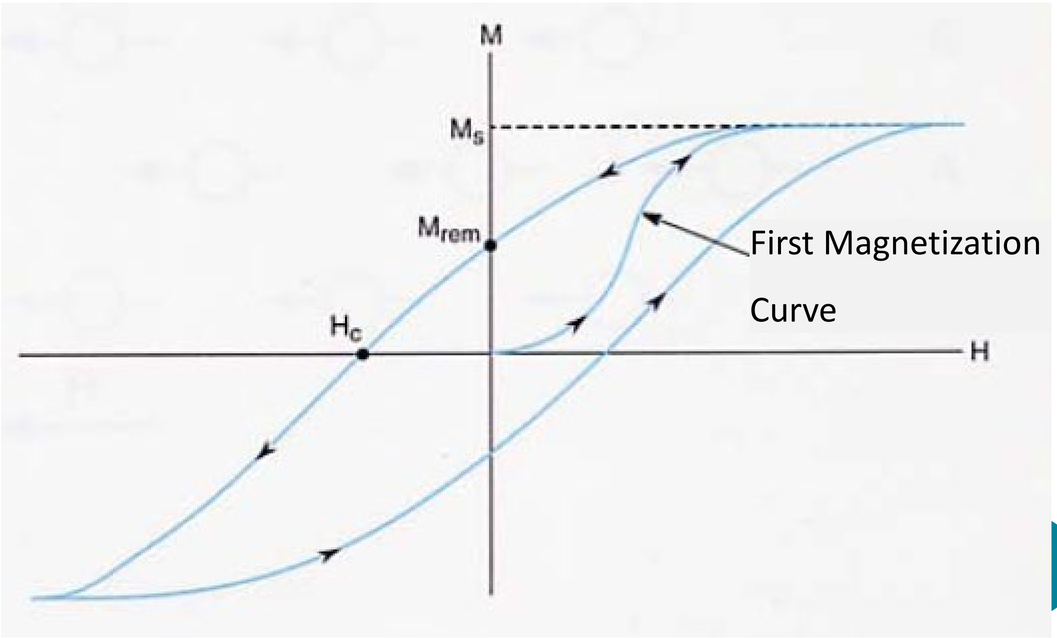

Magnetic Permeability μ

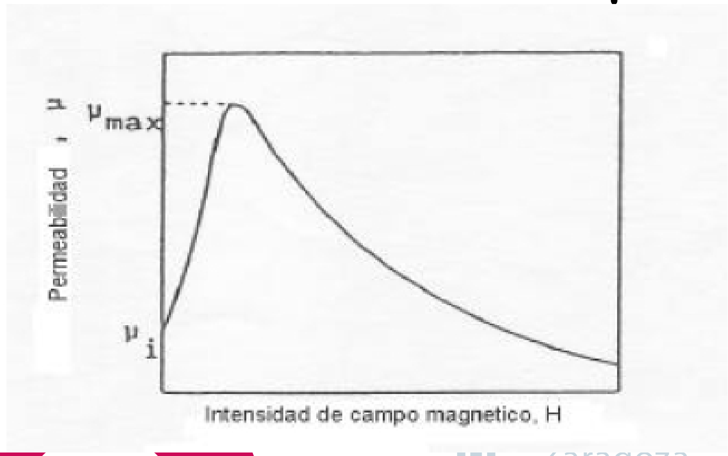

Magnetic Properties of Materials

Antiferromagnetism

•In an AF material neighbour magnetic moments align antiparallely canceling each other :

- Very low M values
- Linear M(H) similar to a paramagnet
- X is a valid property

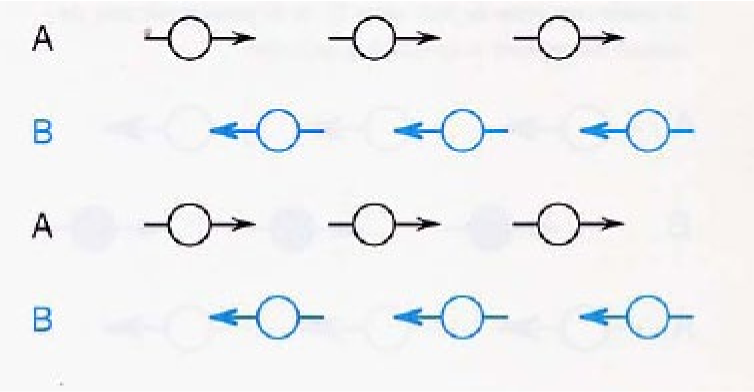

Ferrimagnetism

•In a Ferrimagnet, neighbour mometns are alligned antiparallely same as in a AF, but they do not cancell each other: Similar behavior to a FM

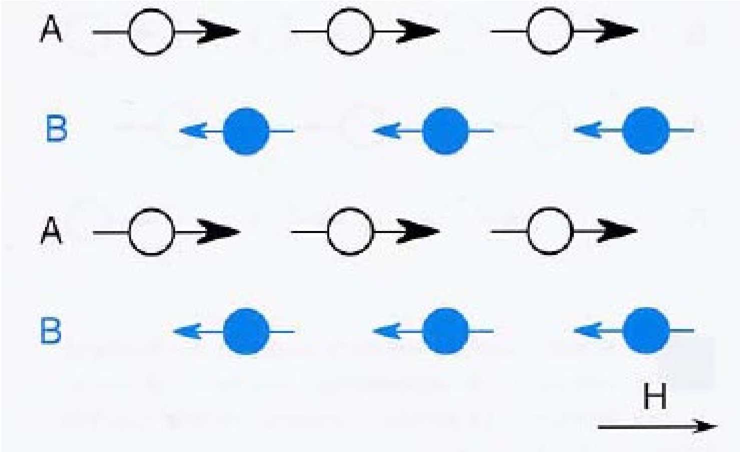

Magnetic Properties of Materials

Ferromagnetism: Magnetic domains, anysotropy

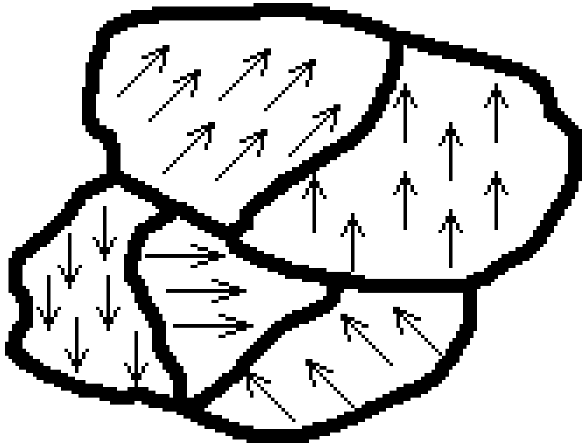

Magnetic Anisotropy

- Crystalline ⇒ SO and Crystal field coupling
- Magnetoelastic ⇒ by deformation
- Shape ⇒ Demagnetizing field

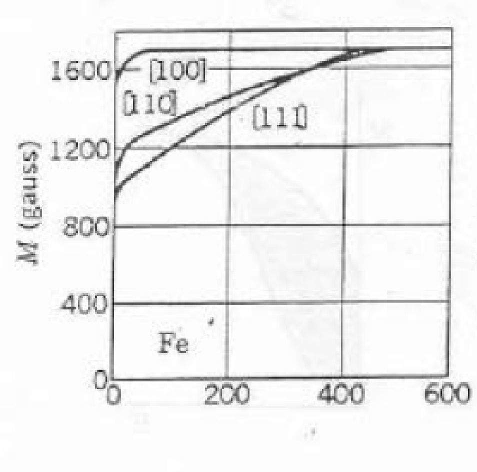

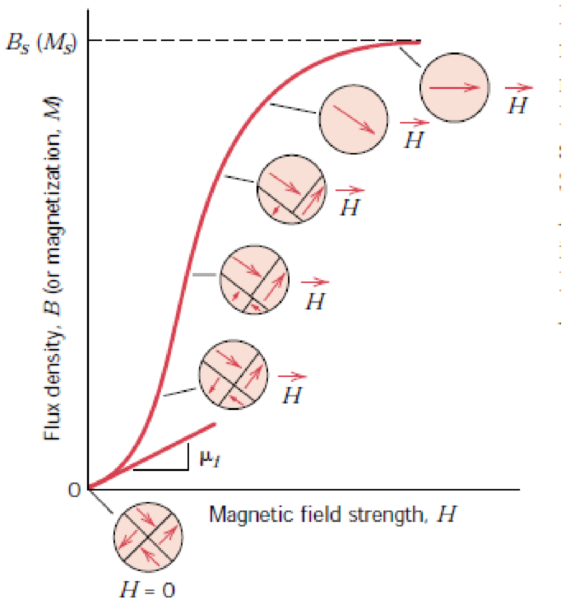

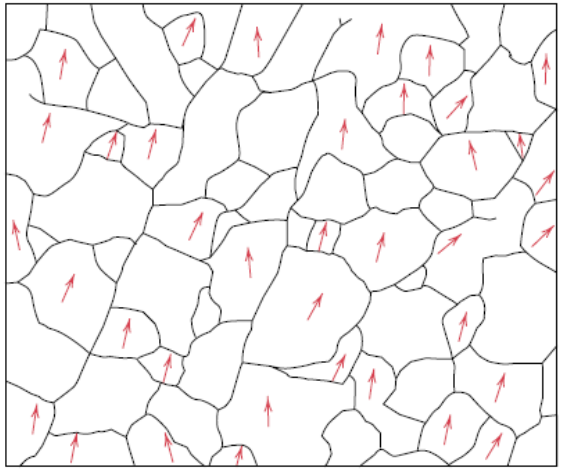

Grain structure of a high-density magnetic storage); the arrows in some of the grains indicate the texture, or the direction of easy magnetization.

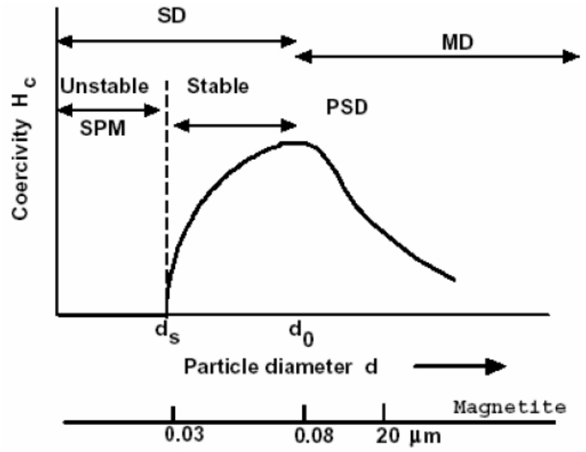

Magnetic Properties of Materials

ASTM Standards

American society for testing and materials

standard ASTM A342, method 5

Standard Test methods for permeability of **weakly magnetic materials** $\mu_r < 6.0$

IEC International Electrotechnical Commission)

INTERNATIONAL

STANDARD IEC 60404-5

Magnetic materials –

Part 5: **Permanent magnet (magnetically hard) materials** – Methods of measurement of magnetic properties

Tumanski, S. (2011). Handbook of Magnetic Measurements (1st ed.). CRC Press. https://doi.org/10.1201/b10979

Magnetic Properties of materials: NITRONIC 50

Magnetic permeability: **M(*T*,*H*), μ(*T*,*H*)**

Physical properties of NITRONIC 50®
Limited magnetic permeability μ ≤ 1.03
Cryogenic temperatures

Magnetic susceptibility of this austenitic Fe-Cr-Ni alloy peaks at approximately 53.5 K (AF transition)

Delta ferrite (bcc **FM**) may form during solidification of steels and welds, remaining stable at all T

Single Piece Forged, SPF

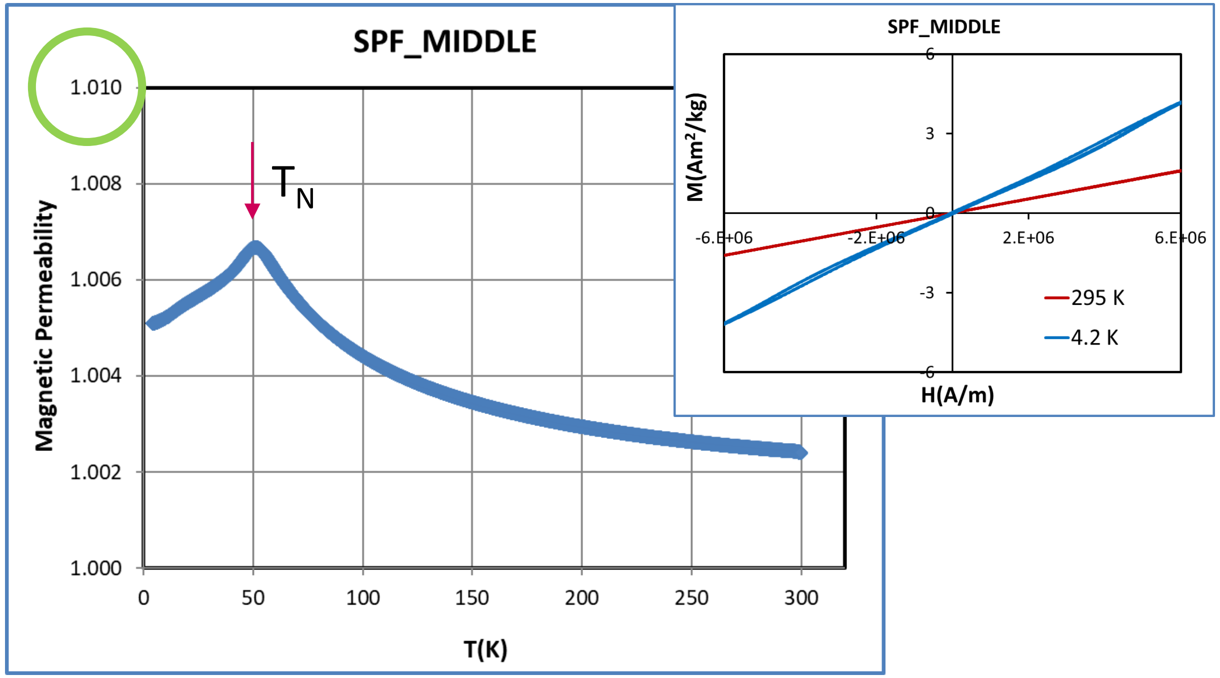

Welded Solution

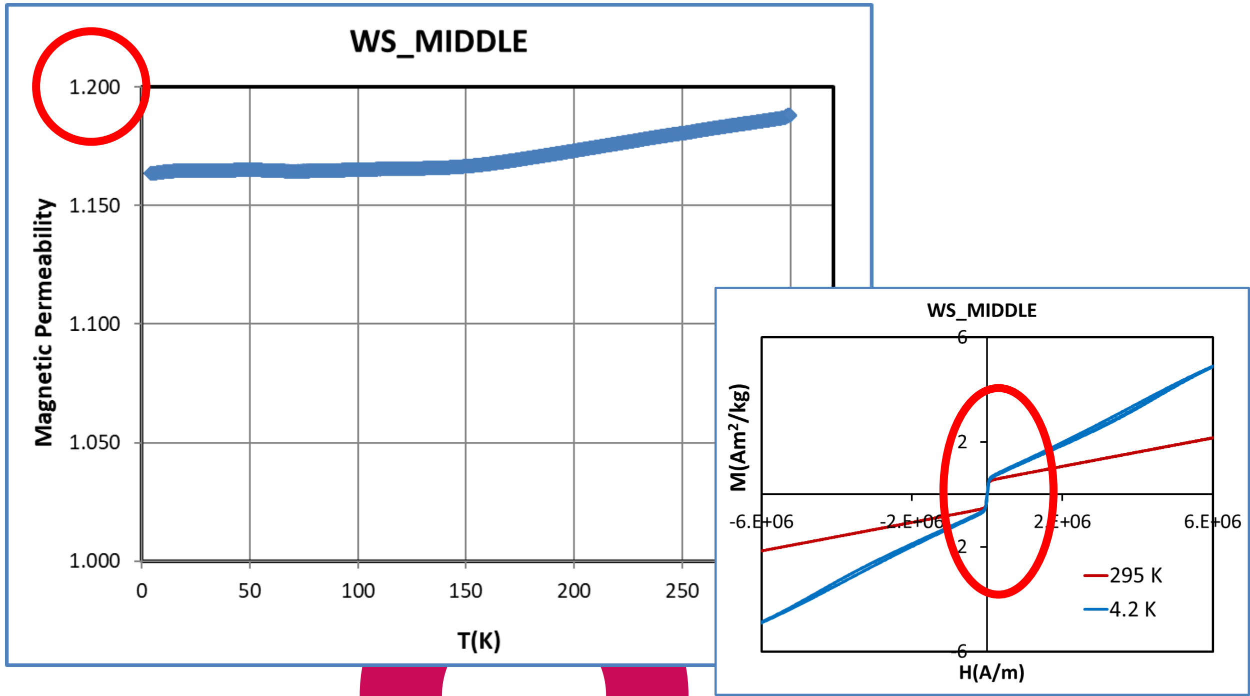

Magnetic Properties of Materials: examples

Non-magnetic Tungsten heavy Alloy material.

ρ = 17 - 19g/cm$_3$

Inermet® 180 Tungsten Heavy Alloy (IT180)
tungsten content (> 90%) and a NiCu binder phase

High-density alloys used in the shielding of the **ITER** (International Thermonuclear Experimental Reactor) fusion reactor.

$\mu_r\,(T,H)$

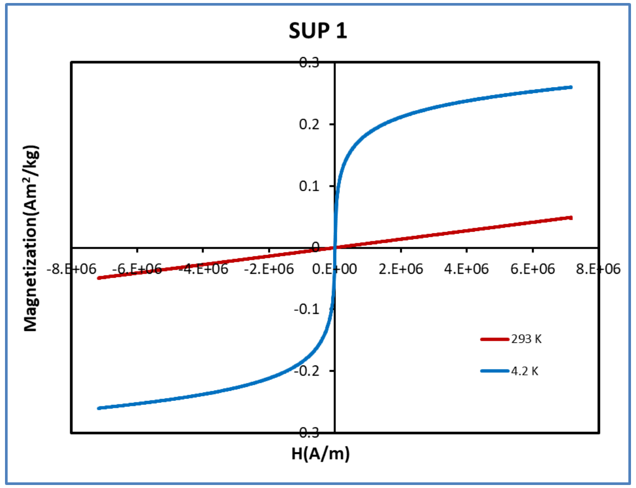

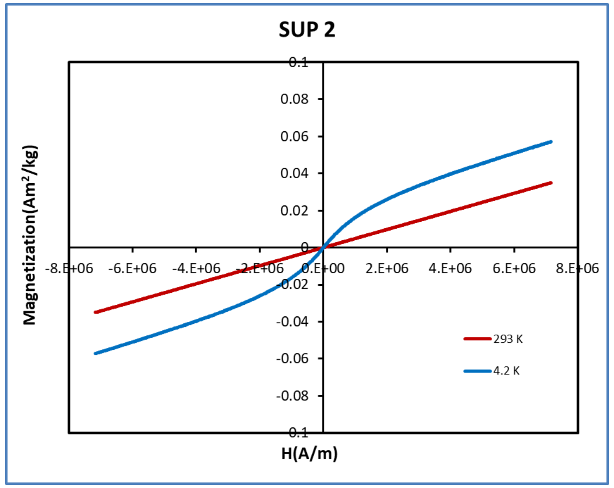

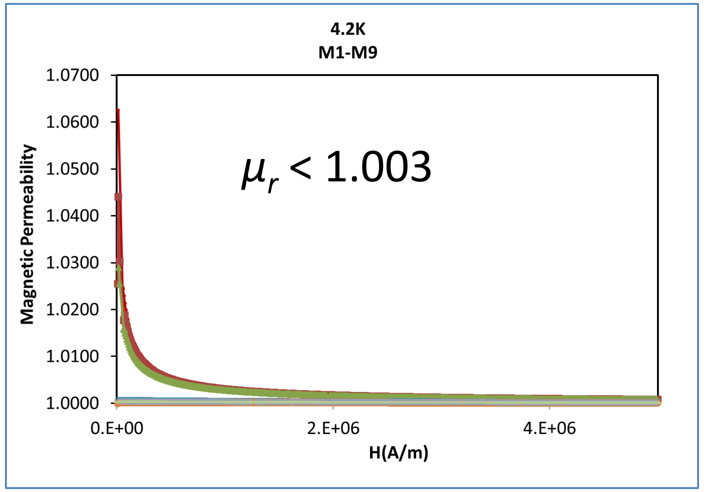

material from different suppliers

Tungsten alloy is used across a range of industries as a shield against gamma and x-ray radiation or as a collimator to focus radiation beams onto a target. With a density 60% greater than lead, it offers superior attenuation characteristics and allows the thickness of shielding to be reduced

Magnetic Properties of Materials

non-magnetic copper alloys

Permeability at a fixed temperature of 1.9K as a function of magnetic field up to *H* = 11,141 kA/m (14 T).

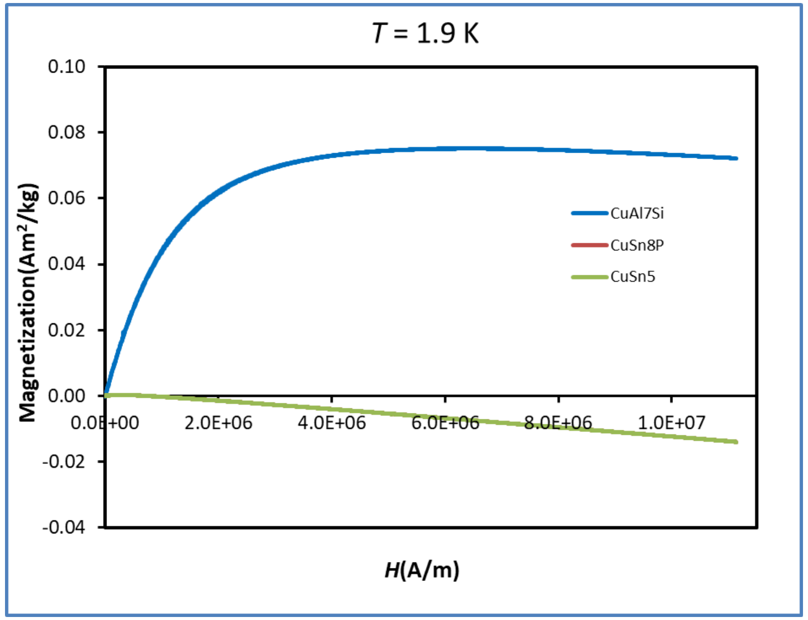

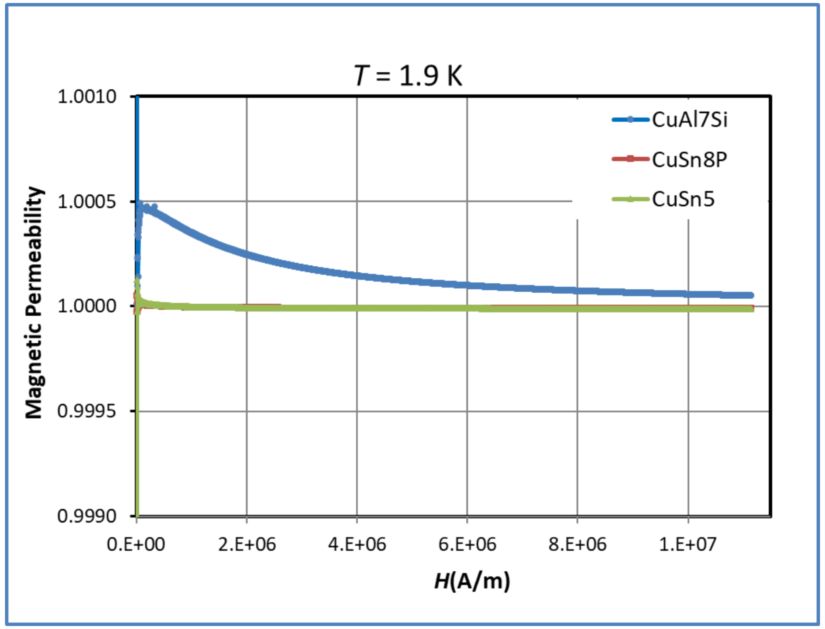

CuAl7Si ⇒ magnetic impurities
CuSn8P ⇒ Diamagnetic
CuSn5 ⇒ Diamagnetic

CERN Project
FCC Future Circular Collider
16T dipole magnets

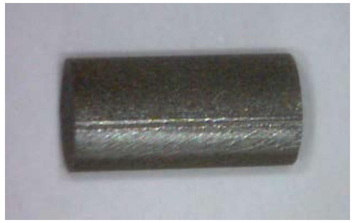

Magnetic Properties of Materials: examples

magnetic steels

FeNi36 alloy magnetic steel (INVAR®)
300-TG-180 microalloyed magnetic steel
500-TG-179 microalloyed magnetic steel
700-TG-178 microalloyed magnetic steel

CERN Project
FCC Future Circular Collider
16T dipole magnets

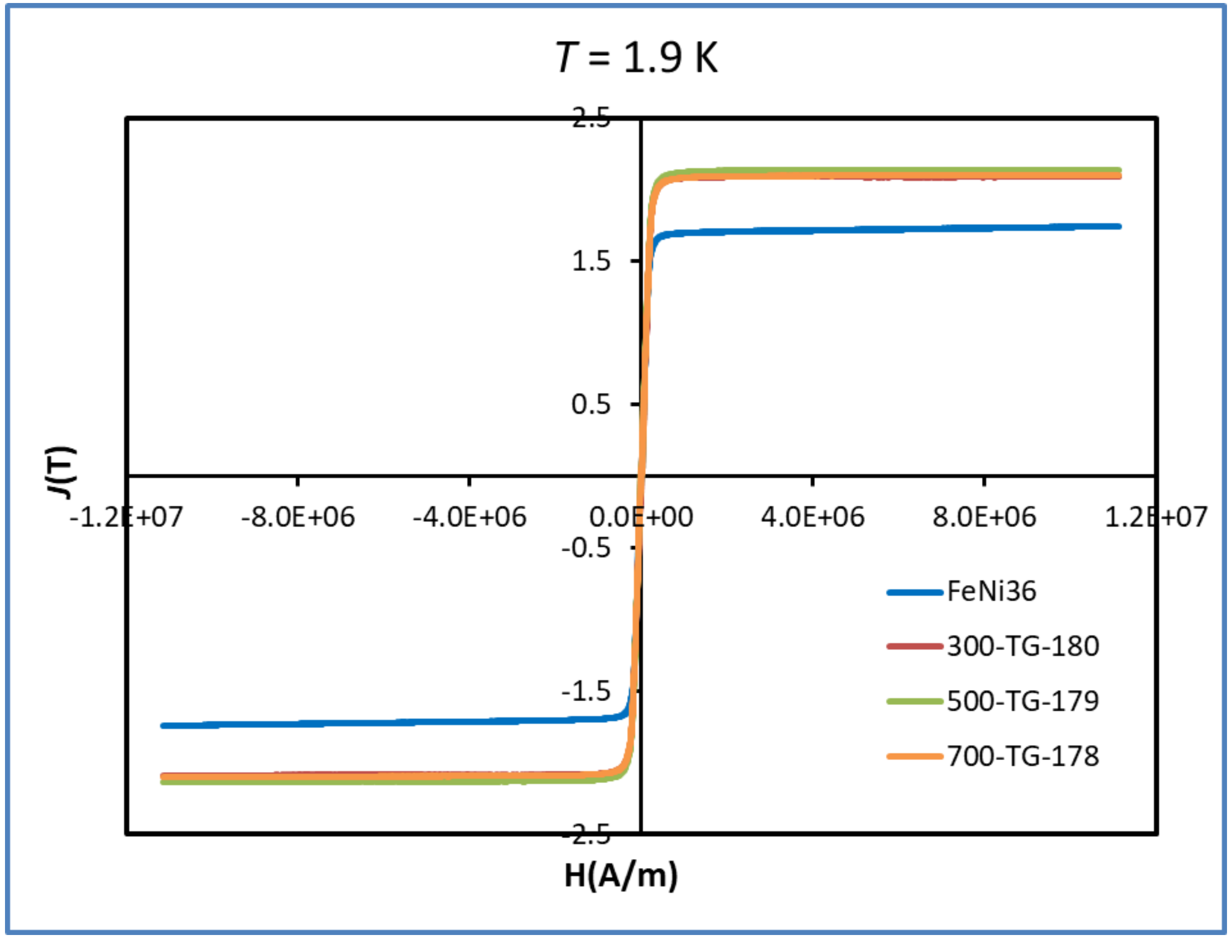

Magnetic polarization saturation

***T* = 1.9 K**
***B* = 14T**

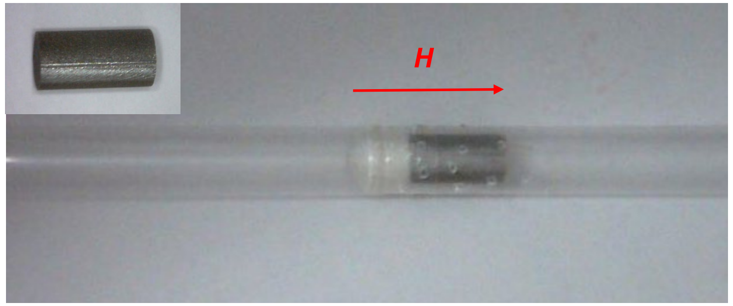

Magnetic Properties of Materials: examples

The CERN Accelerator School

Nanocrystalline Soft magnetic materials
FeSi alloys **FINEMET®**

Nanocrystalline Ribbons of FeSiNbCu
Amorphous Ribbons of FeSiB

Curie Temperature

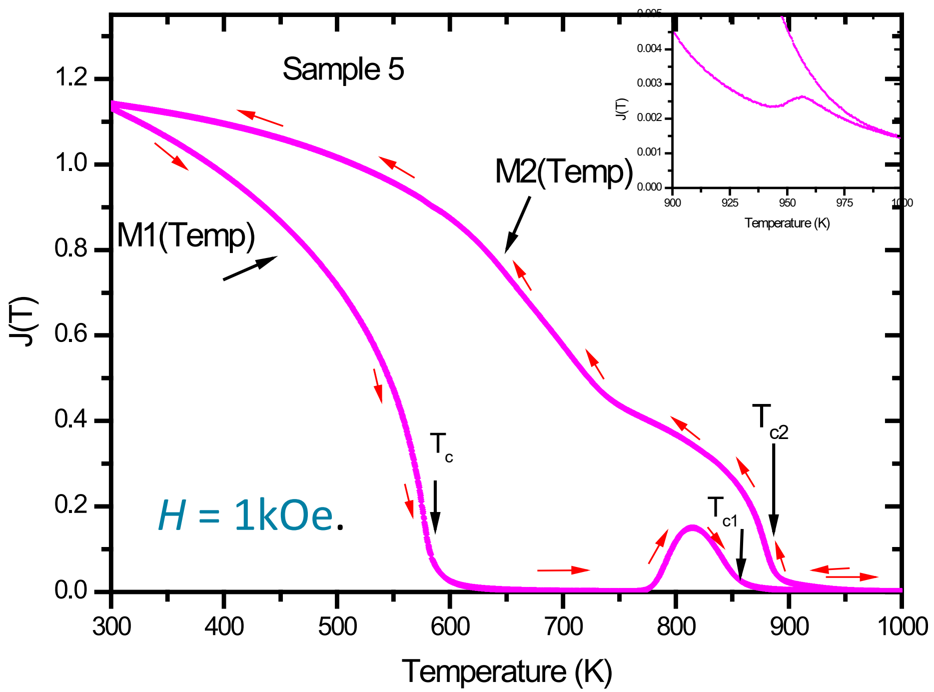

<u>Annealing process of the material</u>

M1(Temp) is the first heating magnetization curve

M2(Temp) successive heating curves

The heating process causes a nanocrystallization of the amorphous alloy

T_c Ferro-paramagnetic transition of the amorphous alloy
T_c1 Curie Temperature from the initial crystalline phase (Fe and Si)
T_c2 Curie Temperature from the main crystalline phase (Fe and Si)

Typical behavior of amorphous magnetic metallic alloys based on the FeSiB system

Universidad Zaragoza

Magnetic Properties of Materials: examples

Non magnetic stainless steel

Austenitic stainless steel sample with partial copper plating and a **longitudinal laser weld** along the center

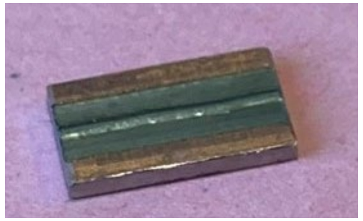

P506 AUSTENITIC STAINLESS STEEL SAMPLE

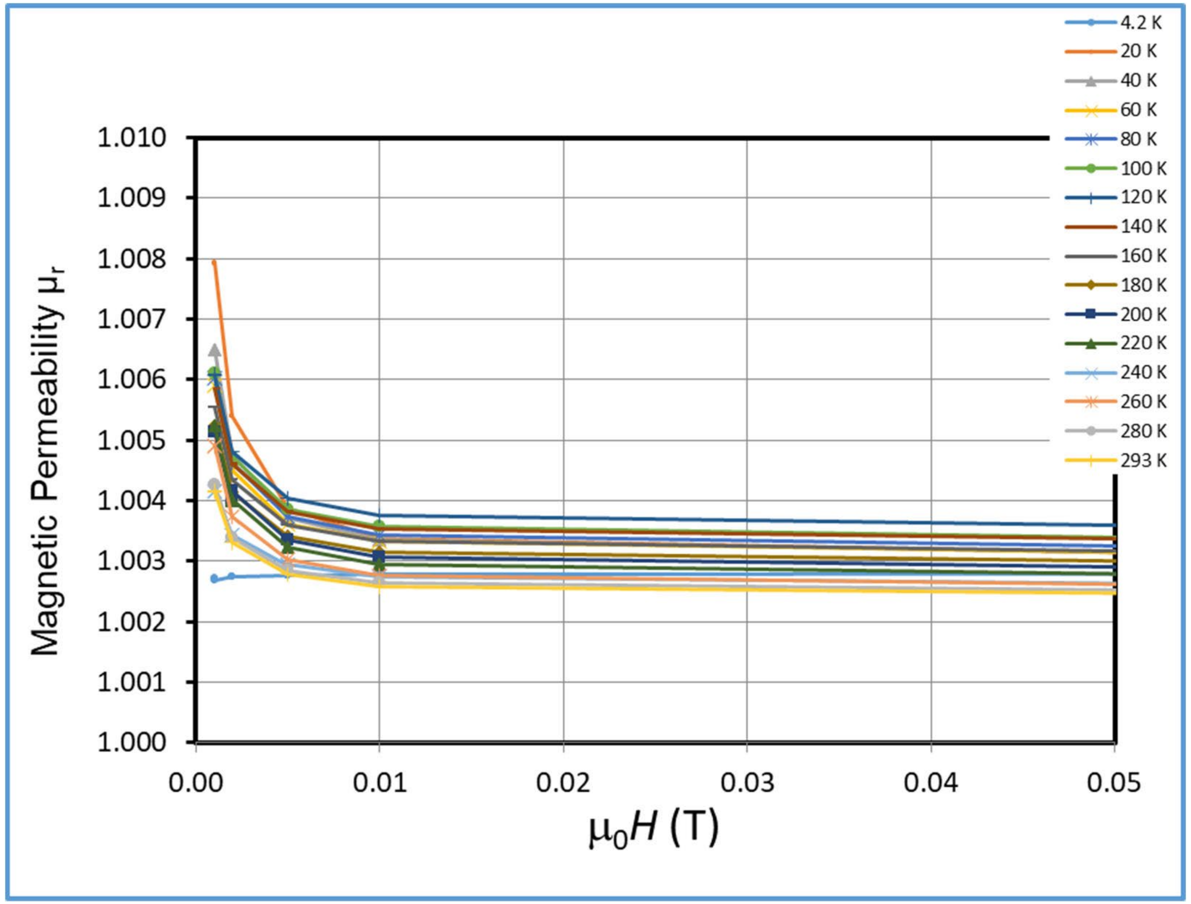

The low field range analysis shows:

- small magnetic remanence
- upturn of permeability

⇓

indicating the presence of magnetic impurities or inclusions in the sample.

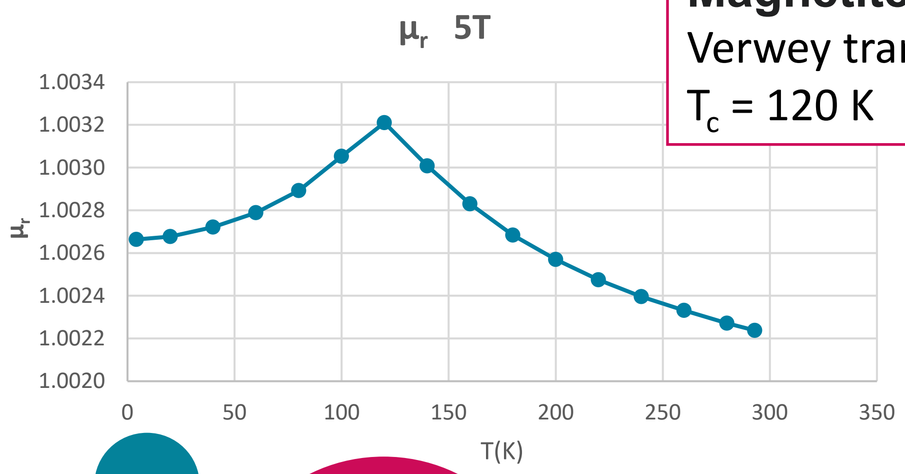

Magnetite Fe_3O_4
Verwey transition
T_c = 120 K

Magnetic Properties of Materials: examples

The CERN Accelerator School

Non magnetic stainless steel

AISI 316

EN 1.4401 – X5CrNiMo17-12-2 (AISI 316)

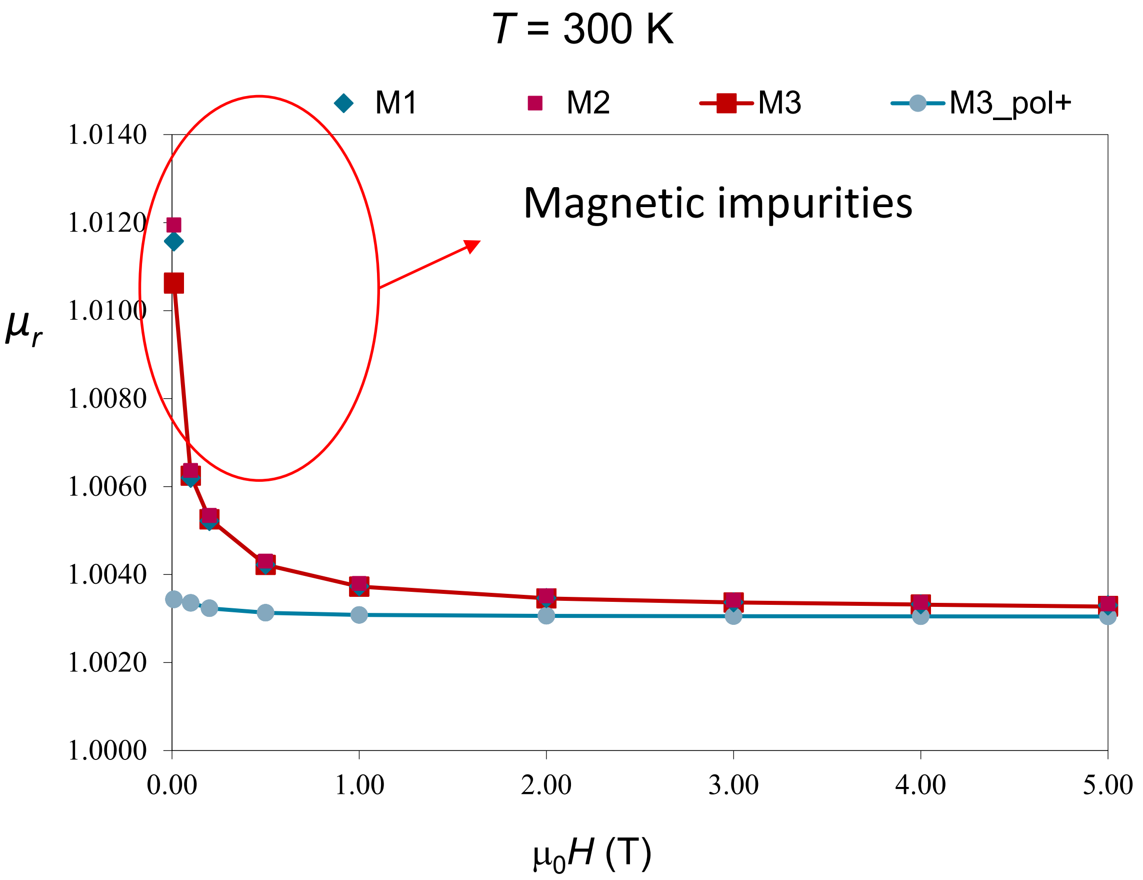

magnetic permeability of non-magnetic AISI 216 steels at room temperature as a function of the magnetic field up to 50 kOe

EDM (Electrical Discharge Machined) cutting process affects the magnetic properties of the sample surface.

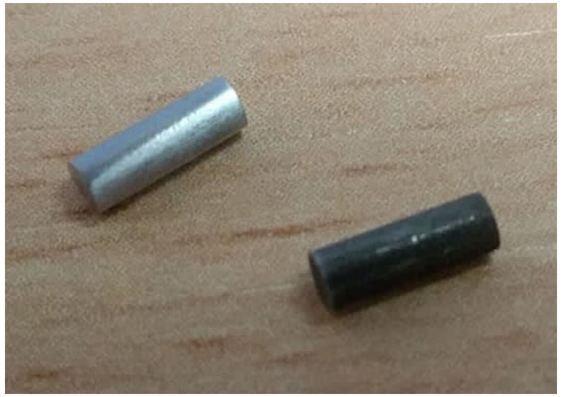

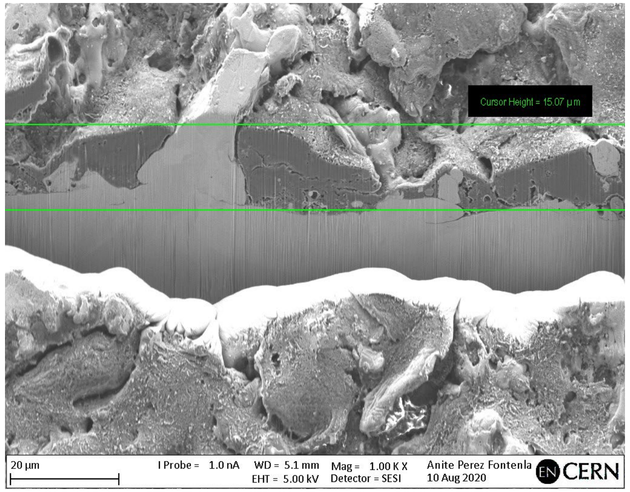

SEM (CERN) image of a FIB section of the surface of one of the samples where the affected surface is visible

Universidad Zaragoza

Summary

The CERN Accelerator School

- Materials for particle accelerators are working under extreme physical conditions: *T*, *H*, *P*, radiation
- Physical Properties of materials change with *T*, *H*.
  - $R(T)$
  - $c_P(T,H)$, $k(T)$
  - $\mu_r(\mathrm{T},H)$
- Materials physical characterization at low *T* and/or high magnetic fields are required to asses requirements (technical specifications) for the final application.
- Advanced study of materials in extreme conditions provides additional fundamental information (phase transitions and stability, thermodynamics, defects, processing of materials, …)

Universidad Zaragoza
1542

Dr. Ana Arauzo
CERN CAS MME for PAD
2 June 2024

aarauzo@unizar.es

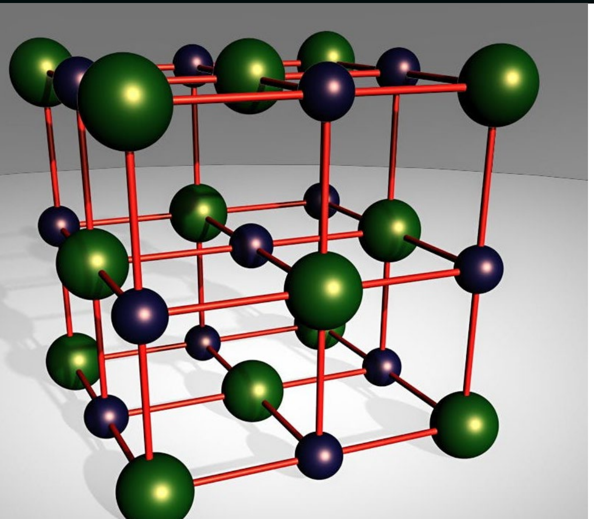

Thank you for your attention

Universidad Zaragoza